

**Gene expression phylogenies and ancestral transcriptome
reconstruction resolves major transitions in the origins of pregnancy**

Katie Mika^{1,2}, Camilla M. Whittington³, Bronwyn M. McAllan^{3,4}, and Vincent J. Lynch^{5,*}

¹ Department of Human Genetics, The University of Chicago, 920 East 58th Street, CLSC 319C,
Chicago, IL 60637, USA.

² Current address: Department of Organismal Biology and Anatomy, University of Chicago,
1025 E 57th Street, Chicago, IL, 60637, USA

³ School of Life and Environmental Sciences, University of Sydney, Sydney, NSW 2006,
Australia

⁴ Charles Perkins Centre, University of Sydney, Sydney, NSW 2006, Australia

⁵ Department of Biological Sciences, University at Buffalo, SUNY, 551 Cooke Hall, Buffalo, NY,
14260, USA.

*Correspondence: vjlynch@buffalo.edu

Abstract

Structural and physiological changes in the female reproductive system underlie the origins of pregnancy in multiple vertebrate lineages. In mammals, the glandular portion of the lower reproductive tract has transformed into a structure specialized for supporting fetal development. These specializations range from relatively simple maternal nutrient provisioning in egg-laying monotremes to an elaborate suite of traits that support intimate maternal-fetal interactions in Eutherians. Among these traits are the maternal decidua and fetal component of the placenta, but there is considerable uncertainty about how these structures evolved. Previously we showed that changes in uterine gene expression contributes to several evolutionary innovations during the origins of pregnancy (Marinic, Mika, and Lynch 2021). Here we reconstruct the evolution of entire transcriptomes ("ancestral transcriptome reconstruction") and show that maternal gene expression profiles are correlated with degree of placental invasion. These results indicate that an epitheliochorial-like placenta evolved early in the mammalian stem-lineage and that the ancestor of Eutherians had a hemochorial placenta, and suggest maternal control of placental invasiveness. These data resolve major transitions in the evolution of pregnancy and indicate that ancestral transcriptome reconstruction can be used to study the function of ancestral cell, tissue, and organ systems.

Introduction

Studies of the fossil record have revealed in fine detail major stages in the origin and diversification of evolutionary novelties (structures) and innovations (functions) such as the vertebrate limb and skull (Abzhanov, 2015; Hirasawa and Kuratani, 2015), the turtle shell (Lyson and Bever, 2020), feathers (Chen et al., 2015), and flowers (Chanderbali et al., 2016). Many features of soft tissues and macromolecular structures, however, are lost during the fossilization process and thus leave little to no trace in the fossil record. To reconstruct the history of these characters, including DNA and amino acid sequences, morphology, physiology, and behavior, among others, evolutionary studies have traditionally relied on comparative (phylogenetic) methods such as parsimony or model-based maximum likelihood or Bayesian inference (Lewis and Olmstead, 2001). These methods infer ancestral characters from the distribution of character states among extant species, the latter of which also allows increased model complexity including unequal character state transitions (Lewis and Olmstead, 2001; Pagel, 1999), variable rates among sites and branches (Galtier, 2001; Yang, 1994, 1993), and character dependent diversification (Maddison et al., 2007).

Extant mammals span crucial transitions in the origins of pregnancy (**Figure 1A**) and are an excellent system in which to explore the origins of evolutionary novelties. The platypus and echidna (monotremes), for example, are oviparous (egg-laying) but retain the egg in the glandular portion of uterus for about two weeks. During this period the developing embryo is nourished by uterine secretions (matrotrophy) delivered through a simple yolk sac placenta (Hughes and Hall, 1998; Renfree and Shaw, 2013). Viviparity (live-birth) evolved in the stem-lineage of therian mammals, but marsupials and eutherians have very different reproductive strategies, particularly in the ontogenetic origins of the definitive placenta and the arrangement of the maternal-fetal interface (Freyer and Renfree, 2009; Renfree and Shaw, 2013; Renfree, 2010). In most marsupials, the embryonic portion of the placenta is derived from the yolk sac, which may come into direct contact with but does not invade the maternal endometrium. While the yolk sac has essential functions during early pregnancy in eutherians, the definitive placenta is derived from chorion and allantois (chorioallantois) and varies in its degree of endometrial invasion (Swanson and Skinner, 2018)(**Figure 1B**). Thus, matrotrophy and a yolk-sac derived placenta were present in the mammalian stem-lineage and transitioned to a chorioallantoic placenta in eutherians.

Unfortunately, most characters related to pregnancy and the nature of the maternal-fetal interface leave little to no trace in the fossil record. Thus, studies exploring the evolution of pregnancy have relied on comparing morphological differences between extant mammals to reconstruct the steps in the origins of pregnancy. These comparative analyses have used multiple methods to reconstruct the arrangement of the mammalian maternal-fetal interface and reached contradictory conclusions about the degree of placental invasiveness in the eutherian ancestor, a debate which has persisted since at least 1876 (**Table 1**). Here, we use comparative transcriptomics and maximum likelihood to infer ancestral gene expression states (ancestral transcriptome reconstruction) from 23 amniotes with different parity modes and degrees of placental invasion to identify the evolutionary history of the maternal-fetal interface. We found strong evidence that the last common ancestor of eutherian mammals had an invasive hemochorial placenta, as well as convergence in gene expression profiles during the independent evolution of non-invasive epitheliochorial placentas in marsupials and some eutherian lineages. These data indicate that the degree of placental invasion can be inferred from endometrial gene expression profiles, and suggest that placental invasiveness is regulated by gene expression profiles in the maternal endometrium rather than the fetal portion of the placenta.

Table 1. Inferences of placental invasiveness in the eutherian ancestor 1880-2021. Note that we follow Mossman (Mossman, 1937, p. 156) and define a placenta as “any intimate apposition or fusion of the fetal organs to the maternal (or paternal) tissues for physiological exchange.”

Study	Data	Method(s)	State
(Turner, 1876)	–	Ontogeny	Epitheliochorial
(Haeckel 1883)	–	Ontogeny	“Non-Invasive”
(Minot, 1891)		Ontogeny	Hemochorial
(Wislocki, 1929)	–	Implicit Parsimony?	Hemochorial
(Hill, 1932)	–	Ontogeny	Epitheliochorial
(Mossman, 1937)		Ontogeny	Endotheliochorial
(Portmann, 1938)	–	Ontogeny	Hemochorial
(Martin, 1969)	–	Ontogeny / Implicit Parsimony	Endotheliochorial
(Kihlström, 1972)	–	Gestation length / Placenta-type Correlation	(Endothelio/hemo)chorial
(Luckett, 1976, 1975, 1974)	–	Ontogeny	Epitheliochorial
(Carter and Enders, 2004)	14 taxa	Ontogeny / Implicit Parsimony	Endotheliochorial
(Vogel, 2005)	22 taxa	Implicit Parsimony	Hemochorial
(Elliot and Crespi, 2006)	88 taxa	Maximum Likelihood	Hemochorial
(Mess and Carter, 2006)	36 taxa	Maximum Parsimony	(Endothelio/hemo)chorial
(Wildman et al., 2006)	44 taxa	Maximum Parsimony & Maximum Likelihood	Hemochorial
(Martin, 2008)	18 taxa	Parsimony	Endotheliochorial (ordered) or (Endothelio/hemo)chorial (unordered)
(Elliot and Crespi, 2009)	334 taxa	Maximum Parsimony & Maximum Likelihood	(Endothelio/hemo)chorial (MP) or Hemochorial (ML)
(McGowen et al., 2014)	66 taxa	Maximum Likelihood	(Superficial) Hemochorial

Results

Endometrial Gene Expression Profiling

We previously assembled a collection of transcriptomes from the pregnant or gravid uterine endometrium of therian mammals with varying degrees of placental invasiveness, as well as a monotreme (platypus), a bird, as well as viviparous, oviparous, and reproductively bimodal lizards (Marinić et al., 2021). The complete dataset includes expression information for 21,750 genes from 23 species (**Figure 2–source data 1**). Principal Component Analysis (PCA) based on gene expression levels in transcripts per million (TPMs), using a variant of PCA that extends PCA to binary data, generally grouped species randomly (**Figure 2A**), consistent with noise in gene expression data overwhelming phylogenetic signal. Therefore, we transformed quantitative gene expression values in transcripts per million (TPM) into discrete character states – Genes with $\text{TPM} \geq 2.0$ were coded as expressed (state=1), genes with $\text{TPM} < 2.0$ were coded as not expressed (state=0), and genes without data in specific species coded as missing (?) (Marinić et al., 2021; Mika et al., 2021). In contrast to PCA based on TPM values, PCA of the binary encoded endometrial transcriptome dataset grouped species by phylogenetic relatedness (**Figure 2B**), indicating significant noise reduction in the binary encoded dataset.

Phylogenetic analyses of endometrial transcriptomes

We used IQ-TREE to infer the best fitting model of character evolution and the maximum-likelihood (ML) phylogeny. The best-fit model of character evolution was a general time reversible model for binary data (GTR2) with character state frequencies optimized by maximum-likelihood (FO) and rate heterogeneity across sites accommodated with the FreeRate model that had three rate categories (R3). Next, we assessed the tree topology and branch support metrics for the ML phylogeny inferred using the binary encoded endometrial gene expression dataset and the GTR2+FO+R3 model. The ML phylogeny (**Figure 3A**) generally followed taxonomic relationships (**Figure 3B**), however, four particularly discordant relationships within therian mammals were inferred with high support: 1) Rather than grouping marsupials into a monophyletic sister-clade to the eutherians, opossum and wallaby were placed as sister-species within the Boreoeutheria; 2) Armadillo groups within the Euarchontoglires rather than as sister to all other eutherians; 3) Bat groups within the Euarchontoglires rather than within Laurasiatheria; and 4) Dog groups within the Euarchontoglires rather than with Laurasiatheria (**Figure 3A/B**). We also used multiple non-parametric topology tests to directly compare the ML tree to alternative trees with the correct phylogenetic placement of these four discordant

lineages, all of which rejected alternative “corrected” trees in favor of the (**Figure 3C**). Remarkably while these discordant relationships are incorrect with respect to the species phylogeny, they are correct with respect to placenta-type, i.e., species form well-supported clades based on their degree of placental invasiveness: Wallaby and opossum, which have epitheliochorial placentas similar to ungulates forms a clade with ungulates, Armadillo, which has an invasive placenta (Carter and Enders, 2004; Chavan and Wagner, 2016), forms a clade with the other species with hemochorial placentas, and dog, which has an invasive endotheliochorial placenta, forms a clade with Euarchontoglires that have invasive hemochorial placentas.

Ancestral transcriptome reconstruction and fuzzy C-Means clustering

We also used IQ-TREE and the species phylogeny (**Figure 3B**) to reconstruct ancestral gene expression states for each gene (ancestral transcriptome reconstruction). To explore the similarity of extant and reconstructed transcriptomes we used Fuzzy C-Means (FCM) clustering, a “soft” clustering method that allows each sample to have membership in multiple clusters and assigns samples to clusters based on their degree of cluster membership. FCM with two to four clusters (K=2-4) had a clear biological interpretation (**Figure 4**): 1) K=2 clustered eutherians and non-eutherians; 2) K=3 clustered most therians with non-invasive (epitheliochorial) placentas, eutherians with invasive (endotheliochorial or hemochorial) placentas, platypus and sauropsids (i.e. viviparous and oviparous lizards, and birds); 3) K=4 clustered eutherians with invasive placentas, eutherians with epitheliochorial placentas, opossum/wallaby, and sauropsids. A notable exception with K=3-4 is the cluster membership of dunnart, which is discussed in greater detail below. FCM clusters with K=5 and K=6 were similar to K=4, but divided Eutherians with hemochorial placentas into two clusters, and clustered dog, dunnart, and the viviparous skink *Chalcides ocellatus* (**Figure 4**); Beyond K=6 clusters had no clear biological interpretation.

Ancestral transcriptome reconstructions generally clustered with extant species having similar parity modes and degrees of placenta invasiveness (**Figure 4**). For example, FCM with K=2 grouped extant eutherians and their ancestral lineages as well as extant non-eutherians and their ancestral lineages. Similarly, FCM with K=4 grouped extant eutherians with invasive placentas and their ancestral lineages with extant therians with non-invasive placentas and their ancestral lineages. FCM with K=3–5 clustered the ancestral eutherian (AncEutheria) transcriptome with extant species that have invasive hemochorial placentas and clustered the

ancestral therian (AncTheria) and mammalian (AncMammalia) transcriptomes with extant mammals that have non-invasive epitheliochorial placentas. These data suggest that FCM clustering of extant and ancestral reconstructions of endometrial transcriptomes can predict ancestral placenta invasiveness, implying that an epitheliochorial placenta evolved early in the development of mammalian pregnancy and that a hemochorial placenta is ancestral for eutherians.

While FCM clustering generally groups extant and ancestral transcriptomes by phylogenetic relatedness and degree of placental invasiveness, a notable exception is the marsupial fat-tailed dunnart (*Sminthopsis crassicaudata*). FCM clusters with K=2–5 grouped dunnart with non-therians while FCM K=6 clustered dog, dunnart, and the skink, *C. ocellatus* (**Figure 4**). FCM cluster membership coefficients of all three species with K=2–5 were mixed, with significant membership across clusters. In contrast, dog, dunnart, and *C. ocellatus* formed a distinct cluster from all other species at K=6 with nearly 100 % FCM cluster membership in group 6 (**Figure 4**). Remarkably, both dog and dunnart have endotheliochorial placentas whereas the *Chalcides* maternal-fetal interface has been described as either endotheliochorial or epitheliochorial with extensive vascularization and interdigitating folds of hypertrophied uterine and chorioallantoic tissue (Blackburn, 1993; Blackburn and Callard, 1997; Corso et al., 2000). These data suggest that species with endotheliochorial placentas have a gene expression profile that is intermediate between epitheliochorial or hemochorial placentas, yet is also distinct, and that gene expression at the *Chalcides* maternal-fetal interface are converging on a therian-like endotheliochorial pattern.

Convergent loss of *RORA* in species with epitheliochorial placentas

Among the genes with discordant species- and gene-expression phylogenies is *RAR-related orphan receptor alpha* (*RORA*), an orphan nuclear hormone receptor that regulates the development and function of type 2 and type 3 innate lymphoid cells (ILC2 and ILC3), which negatively regulates the immune system in local microenvironments especially during inflammation (Haim-Vilmsky et al., 2020), the establishment of tolerance to intestinal microbiota (Lyu et al., 2022), and the regulation of inflammatory responses and vascular remodeling during placentation and pregnancy (Balmas et al., 2018; Mendes et al., 2020; Miller et al., 2018). Remarkably *RORA* independently lost endometrial expression at least four times, each loss coincident with the independent evolution of non-invasive epitheliochorial placentas (**Figure 5A**). The restricted expression of *RORA* to immune cells in the human first trimester

decidua (Vento-Tormo et al., 2018) (**Figure 4B**) suggests that the repeated loss of *RORA* expression reflects changes in the composition of immune cells at the maternal-fetal interface in species with epitheliochorial placentas. To explore this possibility, we used CIBERSORT to deconvolve endometrial bulk RNA-Seq datasets from each species into cell-type abundance estimates with a signature gene expression matrix composed of cell-types from the human first trimester maternal-fetal interface. We found that CIBERSORT inferred that nearly all species that lacked *RORA* expression also lacked ILC2/3 cells at the maternal-fetal interface with the exception of armadillo and chicken which had *RORA* expression but were inferred to lack endometrial ILC2/3 cells, and the viviparous *Saiphos* population which has an epitheliochorial placenta and *RORA* expression and was inferred to have a population of ILC2/3 cells. Thus, we conclude that there is convergent loss of *RORA* in species with epitheliochorial placentas which in many species correlates with the convergent loss of ILC2/3 cells at the maternal-fetal interface.

Discussion

One of the central goals of DevoEvo is a mechanistic explanation for the origin and evolution of evolutionary novelties (Amundson, 2005; Brigandt and Love, 2010; Lynch, 2022; Wagner, 2001, 2000; Wagner and Larsson, 2003). A major challenge for reconstructing the origins of evolutionary novelties, however, is a lack of transitional forms among living species. For example, while feathers and the turtle's shell are excellent examples of morphological novelties, there are no living species with transitional forms between scale and feather (Chen et al., 2015) or with protoshells (Lyson and Bever, 2020). Despite the lack of transitional forms among extant taxa, an abundance of fossil data has reconstructed the major steps in the evolution of these structures that when combined with molecular studies of their development provides a rich explanation for their developmental evolution. Unfortunately, many features of soft tissues leave little to no trace in the fossil record, thus the steps in their evolution have remained elusive. Here we used ancestral transcriptome reconstruction to trace gene expression changes during the origins of mammalian pregnancy, in which extant species preserve intermediate stages in the evolution of both pregnancy and a diversity of placenta types and reconstruct the evolution of placental invasiveness of ancestral species.

Binary encoding uncovers hidden biological signal

While transforming gene expression count data into binary categories likely loses information about evolutionarily relevant variation in expression levels, it may not be possible to

infer meaningful gene expression levels from bulk RNA-Seq. For example rather than evolutionary differences between individuals or species, variation in transcript abundance between samples can result from various sources of experimental noise such as technical variation in library preparation, sequencing, or batch effects (Gilad and Mizrahi-Man, 2015; Tung et al., 2017), variation in cell-type composition of a tissue (Price et al., 2022), sampling different timepoints in development or only a few individuals that do not capture the variance properties of gene expression levels within a population or species (Pal et al., 2021; Thompson et al., 2020). Thus, by transforming gene expression data into not/expressed states we may reduce the potential for these and other biases to influence our ancestral transcriptome reconstructions, revealing biological signal. Our binary encoded endometrial gene expression dataset, for example, cluster species with similar placenta types and parity mode (**Figure 2B**) indicating binary encoding preserves functional signal in gene expression data that is otherwise masked by variation in gene expression levels (**Figure 2A**).

Phylogenetic analyses of endometrial transcriptomes

Previous studies of molecular phylogenies have shown that gene-species tree discordance can result from convergent or parallel amino acid changes in lineages that independently evolved morphological traits. For example, parallel amino acid changes in *prestin* (*SLC26A5*), a motor protein expressed in outer hair cells in the cochlea that essential for hearing, have occurred in different lineages of echolocating mammals, including multiple lineages bats and whales, leading a strongly monophyletic clades in gene trees that do not reflect taxonomic relationships (Li et al., 2008, 2010; Liu et al., 2010; Teeling, 2009). Gene-species tree discordance is also associated coadaptation of amino acid substitutions in Na^+K^+ -ATPase of frogs that prey on toxic toads (Mohammadi et al., 2021), the evolution of *C₄ phosphoenolpyruvate carboxykinases* (*PCK*) in grasses (Christin et al., 2009), and between snake and agamid lizard mitochondrial genomes (Castoe et al., 2009). These examples highlight how phylogenetic discordance can be a signal of convergent evolution, rather than just a sign of biased phylogenetic inference that can arise from processes like long branch attraction (Bergsten, 2005; Felsenstein, 1978), incomplete lineage sorting and introgression (Guerrero and Hahn, 2018; Hibbins et al., 2020; Maddison and Knowles, 2006), biased character state frequencies and gene conversion (Figueta et al., 2014; Kostka et al., 2012; Lartillot, 2013; Romiguier et al., 2013), and heterotachy (Kolaczkowski and Thornton, 2008; Philippe et al., 2005), among others.

Similar to the signals of convergence from gene-species tree discordance, our transcriptomic data showed significant phylogenetic support for uterine transcriptomes grouping by parity mode and degree of placental invasiveness rather than phylogenetic relationships. This transcriptome-species tree discordance is particularly striking for opossum and wallaby, which are deeply nested within eutherians with epitheliochorial placentas based on uterine transcriptome data, because the eutherian and marsupial placenta is derived from different extra-embryonic tissues – the chorion and allantois in eutherians and the yolk-sac in marsupials. Thus, there must be significant convergence in *endometrial* gene expression profiles between eutherians with chorioallantois-derived epitheliochorial placentas and marsupials with yolk-sac epitheliochorial placentas because our transcriptome phylogeny is based on gene expression in the endometrium during pregnancy rather than gene expression in the placenta. This convergence in gene expression between species with non-invasive epitheliochorial placentas may be related to the expression of genes that limit the ability of the trophoblast to invade into maternal tissues (see below).

Reconstruction of ancestral (endometrial) transcriptomes

Previous studies have explored transcriptome evolution with the goal of developing methods of ancestral transcriptome inference (Price et al., 2022), characterizing the general tempo and mode of gene expression evolution (Bauernfeind et al., 2021), implicating transcriptome evolution in the origin and evolution of morphological traits (Church et al., 2022; Katelyn et al., 2021; Lynch et al., 2015; Marinić et al., 2021; Munro et al., 2021), and identifying specific genes with derived expression levels (Brawand et al., 2011; Necsulea et al., 2014), usually in the context of characterizing genes whose expression levels have changed because of the action of positive selection, i.e., directional selection on transcript abundance (Gu, 2004; Price et al., 2022; Yang et al., 2020). In contrast, only a few studies have treated the expression of individual genes as a discrete character, transforming quantitative gene expression levels into binary not/expressed states, and used ancestral state reconstruction to determine the expression state of all genes in an ancestral transcriptome rather than changes in the expression levels of specific genes (Katelyn et al., 2021; Kin et al., 2015; Lynch et al., 2015; Marinić et al., 2021). Our ancestral transcriptome reconstructions of gene expression state indicate that an epitheliochorial-like placenta evolved early in the mammalian stem-lineage, before the loss of the egg-shell in Therians, and that the ancestor of Eutherians had a hemochorial placenta, which resolves a longstanding debate about the nature of ancestral mammalian placentas. These data suggest that ancestral transcriptome reconstruction can be

used to infer the function of ancestral cell, tissue, and organ systems which leave little to no trace in the fossil record even if soft tissues might by chance fossilize.

Convergent loss of *RORA* in species with epitheliochorial placentas

Our observation that *RORA* expression has been lost multiple times in species with non-invasive epitheliochorial placentas, which is coincident with the inferred absence of ILC2/ILC3 cells from the endometrium during at least one stage in pregnancy. This result suggests a mechanistic connection between absence of decidual *RORA* expression, the absence of decidual ILC2/ILC3 cells, and the loss of placental invasion. Indeed, the major decidual ILC produce signaling factors such as GM-CSF, XCL1, MIP1 α , and MIP1 β , whose receptors are expressed by EVT likely regulate placental invasion (Huhn et al., 2020). ILC2 also contributes to the maintenance of a type-2 anti-inflammatory immune environment in the uterus during pregnancy (Balmas et al., 2018), which may be particularly important in species in which the endotheliochorial or haemochorial placenta invades maternal tissues. ILC2s, for example, are increased in the decidua basalis of women with spontaneous preterm labor compared to those who delivered preterm without labor (Mendes et al., 2021; Xu et al., 2018), suggesting that ILCs may participate in the chronic inflammatory process that occurs during pregnancy. Thus, loss of placental invasion may be associated with a reduced need to limit local inflammation by ILCs, leading to an evolutionary loss of ILCs in the endometrium during pregnancy. However, while our data are consistent this role for decidual ILC2 and its association with placental invasion, more detailed studies specifically aimed at characterizing cell-type composition differences across species are necessary to determine if there are correlations between cell-types in the endometrium during pregnancy and placenta type.

Ideas and Speculation: Maternal control of placental invasion

Our observation that endometrial gene expression patterns are correlated with degree of placental invasiveness might seem surprising, however, rather than acting as a passive substrate into which the trophoblast invades, the endometrium directly controls trophoblast invasion (Cui et al., 2012; Graham and Lala, 1991). For example, the trophoblast of mammals with hemochorial placentas, such as humans and rodents, is only permissive to invasion when the “window of implantation” is opened by the endometrium. Similarly, while the trophoblast of mammals with non-invasive endotheliochorial and epitheliochorial placentas, such as cats, dogs, horses, cows, pigs, and sheep cannot invade into the endometrium, they can invade into ectopic sites (reviewed in (Corpa, 2006)). The trophoblasts of guinea pig (Loeb, 1914), mouse

(Billington, 1965), rat (Jollie, 1961), and pig (Samuel and Perry, 1972) also invade ectopic sites in experimentally induced ectopic pregnancy. While there is no similar ectopic pregnancy data for marsupials, some marsupial lineages, including dunnart, have evolved invasive placentation. In contrast, there is no invasion of maternal tissues during ectopic pregnancy in viviparous reptiles with epitheliochorial placentation such as *Pseudemoia entrecasteauxii* (Griffith et al., 2013). Thus, the invasive ability of trophoblasts most likely either evolved in the stem-lineage of therian mammals or multiple times, including in the stem-lineage of eutherians and some lineages of marsupials. Regardless, ancestral maternal control of placental invasion likely allowed us to infer ancestral placental invasiveness from ancestral endometrial transcriptomes.

Ideas and Speculation: Evolution of placental invasion and cancer metastasis

Numerous authors have noted the similarity between placental invasion and cancer metastasis (Costanzo et al., 2018; Ferretti et al., 2006; Kozlov, 2022; Lala et al., 2021; Manzo, 2019; Murray and Lessey, 1999; Perry et al., 2009; Piechowski, 2019), which was first proposed in 1902 by Scottish embryologist John Beard (1858–1924) who hypothesized that ectopic trophoblasts gave rise cancer (Gurchot, 1975; Ross, 2014). While Beard’s hypothesis is incorrect, at least for cancers not derived from the placenta such as choriocarcinoma, there are numerous mechanistic similarities between implantation, placental invasion, and tumor progression to malignancy (Nordor et al., 2017; Wagner et al., 2021). These data suggest that the evolution of maternal mechanisms that prevent endometrial invasion through expression gain and loss of genes that restrain and promote, respectively, trophoblast invasion, may be related to resistance to metastasis in eutherian lineages with non-invasive placentas (Boddy et al., 2020; Kshitiz et al., 2019; Wagner et al., 2020). For example, pleiotropy can lead to correlated patterns of gene expression between the transcriptomes of different tissue and organ systems (Liang et al., 2018). Thus, the evolution of a gene regulatory module that restricts placental invasion into the endometrium can be coopted to restrict implantation and spread of cancer cells into metastatic locations.

Caveats and limitations

A limitation of this study not directly addressed thus far is that we have only sampled a small number of species. For example, we lack pregnant endometrial samples from most

mammals, particularly those with endotheliochorial placentas, as well as a diversity of oviparous and viviparous squamates (there are at least 115 origins of viviparity in squamates (Blackburn, 2015; Blackburn and Brandley, 2015; Blackburn and Starck, 2015). Thus, our inferences from phylogenetic, ancestral reconstruction, and clustering analyses may be biased by small sample sizes and non-random sampling. We also assume that models of evolution designed for phylogenetic inference and ancestral reconstruction of morphological and molecular data are appropriate for gene expression data or binary encoded gene expression data, which may affect our results; for example, we have not directly accommodated incomplete lineage sorting which can mislead phylogenetic inference (Guerrero and Hahn, 2018; Hibbins et al., 2020). Similarly, while Fuzzy C-Means clustering is conceptually similar to topic ("grade of membership") models used in population genetics, its underlying assumptions may be violated for gene expression and binary encoded gene expression data. More detailed studies are necessary to determine if our results are robust to potential sources of error such as model mis-specification, small sample sizes, and non-random taxon sampling, as well as incomplete lineage sorting, the latter of which we were unable to directly test.

Conclusions

Previous critiques of statistical methods to infer ancestral states, particularly in the context of parity mode evolution in squamates, have suggested that ancestral state reconstructions of morphological characters must be supported by additional kinds of biological support such as anatomical, physiological, and ecological evidence, to be persuasive (Griffith et al., 2015). Here we explored the evolution of parity mode and placental invasiveness in amniotes utilizing comparative gene expression data. While our study also relies on statistical methods to infer ancestral (gene expression) states, this approach is orthogonal to traditional methods that infer ancestral states from morphological characters among extant species. Indeed, gene expression ultimately underlies the development, evolution, and function of anatomical systems. Thus, by reconstructing the evolution of entire transcriptomes we may be able to infer function of ancestral cell, tissue, and organ systems. Our results resolve several evolutionary transformations during the origins of pregnancy, including the early evolution of an epitheliochorial-like placenta in the mammalian stem-lineage, a hemochorial placenta in the ancestor of eutherians, multiple reversions to non-invasive epitheliochorial placentas within some eutherian lineages, convergent evolution of gene expression profiles among species with different ontogenetic origins of epitheliochorial placentas, and maternal control of placental invasiveness.

Materials and Methods

Endometrial Gene Expression Profiling

We previously published a dataset of uterine endometrial transcriptomes, which is also used in this study. Interested readers are referred to Mika, Marinic, and Lynch (2021) for specific details. Briefly, we searched the NCBI BioSample, Short Read Archive (SRA), and Gene Expression Omnibus (GEO) databases using the search terms “uterus”, “endometrium”, “decidua”, “oviduct”, and “shell gland”. These anatomical terms refer to the glandular portion of the female reproductive tract, which is specialized for maternal-fetal interactions or shell formation. We then manually curated transcriptomes and excluded those that did not indicate whether tissue samples were from pregnant or gravid tissues and datasets composed of pooled tissues. Gene expression data were analyzed with Kallisto (Bray *et al.*, 2016) version 0.42.4 to pseudo-align the raw RNA-Seq reads to reference transcriptomes and to generate transcript abundance estimates (see **Figure 2–source data 1** for accession numbers and reference genome assemblies); Kallisto was run using default parameters, bias correction, and 100 bootstrap replicates.

Gene expression phylogeny and ancestral transcriptome reconstruction

We used the binary encoded endometrial transcriptome dataset for phylogenetic analyses and to reconstruct ancestral gene expression states. Gene expression phylogenies were inferred with IQ-TREE2 (Nguyen *et al.*, 2015) using the best-fitting model of character evolution determined by ModelFinder (Kalyaanamoorthy *et al.*, 2017). The best fitting model was inferred to be the General Time Reversible model for binary data (GTR2), with character state frequencies optimized by maximum-likelihood (FO), and a FreeRate model of among site rate heterogeneity with three categories (R3) (Soubrier *et al.*, 2012). The rate at which characters evolve may vary over time, with the same character evolving rapidly or slowly in different lineages. This phenomenon, known as heterotachy, can bias phylogenetic trees using models of evolution that assume the rates of character evolution are constant such as the GTR+FO+R3 model. Therefore we compared the GTR2+FO+R3 model to the General Heterogeneous evolution On a Single Topology (GHOST) model; The GHOST model accommodates heterotachy by combining features of mixed substitution rate models (Foster 2004; Lartillot and Philippe 2004; Pagel and Meade 2004), whereby each class of characters

has its own substitution rate matrix, and mixed branch length models (Kolaczowski and Thornton 2004; Meade and Pagel 2008), whereby each class of characters has its own set of branch lengths.

We found the best-fit GHOST model was GTR2+FO*H4 (AICc = 215681.71), which accommodated rate heterotachy with 4 categories, described the binary encoded gene expression dataset better than the standard GTR2+FO+R3 model (AICc = 220930.65) indicating that there is extensive variation in the rate of character evolution over time. However, while there was a significant likelihood difference between GTR2+FO+R3 and GTR2+FO*H4 (AICc difference = 5248.94), as well as other heterotachy with models with less than or more than 4 categories, the topology of the trees was the same. Thus, while accommodating heterotachy improves estimation of parameters of the substitution model it had no affect on the tree topology and we therefore use the computationally simpler GTR2+FO+R3 model for downstream analyses; This is particularly important for non-parametric topology tests and ancestral state reconstructions (discussed below), which as currently implemented in IQ-TREE2 cannot accommodate heterotachy models with unlinked model parameters.

Ancestral gene expression states for each gene were inferred using the empirical Bayesian method implemented in IQ-TREE2, the GTR2+FO+R3 model of character evolution, and the species phylogeny as a constraint tree (**Figure 3B**). Branch support was assessed using the standard (StdBoot) and ultrafast (UFBoot) bootstraps, which assess the effects of sampling bias on branch support (Hoang et al., 2018; Minh et al., 2020). We also used several single branch tests, including the SH-like aLRT and the parametric aLRT (Anisimova et al., 2006; Guindon et al., 2010), aBayes (Anisimova et al., 2011), and the local (LBoot) bootstrap tests (Minh et al., 2020); single branch tests assess whether a branch provides a significant likelihood improvement compared to a null hypothesis that collapses the branch to a polytomy but leaves the rest of the tree topology unaltered. We considered a clade to be highly-supported if its StdBoot support $\geq 80\%$, UFboot $\geq 95\%$, SH-aLRT $\geq 80\%$, aBayes ≥ 0.90 , parametric aLRT ≥ 0.95 , and LBoot $\geq 90\%$ (Anisimova et al., 2011).

The bootstrap and single branch tests assess the robustness of individual branch bipartitions and cannot directly compare complex alternate tree topologies. Therefore we used non-parametric topology tests to directly compare the inferred ML tree to alternative trees with the correct phylogenetic placement of platypus, armadillo, dog, marsupials (opossum and wallaby), and bat, as well as the correct species phylogeny (**Figure 2B**); tests included the BP-

RELL, KH-test (Kishino et al., 1990; Kishino and Hasegawa, 1989), SH-test (Anisimova et al., 2011; Guindon et al., 2010), c-ELW (Strimmer and Rambaut, 2002), weighted KH- and SH-tests, and the AU-test (Shimodaira, 2002). We note that the KH-test compares two *a priori* defined trees rather than the ML and alternative trees (Goldman et al., 2000) and does not correct for multiple hypothesis tests, it is included solely for comparison to other methods and previous studies. The SH-test can be used to compare the ML tree to multiple alternative trees selected *a priori* (i.e., is dataset independent) and corrects for multiple hypothesis tests, but is too conservative when many trees are tested. The AU-test, in contrast, resolves the conservative nature of the SH-test and thus is the preferred test. All tests performed 100,000 resamplings using the RELL method.

Clustering methods

We evaluated multiple methods to summarize and visualize the binary encoded extant and ancestral reconstructed transcriptomes, including: 1) Logistic Principal Component Analysis (LPCA), a version of principal component analysis for dimensionality reduction of binary data (<https://cran.r-project.org/web/packages/logisticPCA/vignettes/logisticPCA.html>); 2) classical Multi-Dimensional Scaling (MDS); 3) Uniform Manifold Approximation and Projection (UMAP); 4) tSNE; and 5) Fuzzy C-Means (FCM) clustering. All clustering analyses were conducted in R after removing columns (genes) with missing data (coded as ?/NA) or that were invariant (all 0 or all 1). LPCA was performed using the `logisticPCA` R package (Landgraf and Lee, 2015), which implements three methods: exponential family PCA applied to Bernoulli data, logistic PCA, and the convex relaxation of logistic PCA. For each of the methods, we fit the parameters assuming two-dimensional representation, returning four principal components ($k_s=4$), and selecting the best m value to approximate the saturated model for cross validation. MDS was performed using the `vegan` R package (Oksanen et al., 2008) with four reduced dimensions. UMAP was performed using the `umap` R package. tSNE was performed using the `Rtsne` R package.

To explore the data in greater detail we focused on FCM clustering because the results were qualitatively similar to the other methods, and it has several desirable properties including providing a statistically sound way to identify clusters rather than an *ad hoc* approach that might be applied to the other methods. FCM also allows each sample to have membership in multiple clusters and is conceptually similar to topic ("grade of membership") models used in population genetics to visualize private and shared genetic structure across populations. FCM membership

coefficients can thereby account for multiple sources of similarity including noise, phylogenetic signal, and convergence of gene expression. FCM was performed in R using the `cluster` R package, using Manhattan distances (cluster membership was not altered by using other distance metrics), and an estimated fuzzifier ($m=1.034978$). FCM clustering requires *a priori* knowledge of the number of clusters (K) to include, therefore we evaluated FCM with K=2–9 following the suggestions given in <https://www.r-bloggers.com/2019/01/10-tips-for-choosing-the-optimal-number-of-clusters/>. First, we used the “elbow” method, in which the sum of squares of each cluster number is calculated and graphed and the optimal number of clusters estimated by a change of slope from steep to shallow (the elbow). We also assessed the optimal number of clusters using the `clustree` R package, which assess the optimal number of clusters by considering how samples change groupings as the number of clusters increases; `clustree` is useful for estimating which clusters are distinct and which are unstable but cannot determine the optimal number of clusters (K).

CIBERSORT analyses

We inferred the proportion of different cell-types in the endometrium during pregnancy across our comparative gene expression datasets using CIBERSORT (Newman et al., 2019), which takes as input a file of gene expression levels from a mixed cell population and a gene expression signature file with expression levels of marker genes in specific cell-types. CIBERSORT was run on the bulk RNA-Seq data from each species using a signature gene expression file based on the Vento-Tormo et al. scRNA-Seq dataset. The signature gene expression file included gene expression data (TPM-like) for genes with an expression level greater than or equal to the expression threshold that also have at least five-fold higher expression levels in a particular cell compared to all other cells (Jain and Tuteja, 2021).

Acknowledgements

The authors would like to thank MB Thompson (University of Sydney) for constructive comments on this manuscript. This study was supported by a grant from the March of Dimes (March of Dimes Chicago-Northwestern-Duke Prematurity Research Center) and a Burroughs Wellcome Fund Preterm Birth Initiative grant (1013760) to principal investigator VJL. The funders had no role in study design, data collection and analysis, decision to publish, or preparation of the manuscript.

511
512
513
514
515
516
517
518
519
520
521
522
523
524
525
526
527
528
529
530
531
532
533
534
535
536
537

References

538 Abzhanov A. 2015. Evolution of the Animal Face: from Principles to Mechanisms. *Faseb J* **29**.
539 doi:10.1096/fasebj.29.1_supplement.867.1

540 Amundson R. 2005. The Changing Role of the Embryo in Evolutionary Thought: Roots of Evo-
541 Devo. Cambridge University Press.

542 Anisimova M, Gascuel O, Sullivan J. 2006. Approximate likelihood-ratio test for branches: A
543 fast, accurate, and powerful alternative. *Systematic Biol* **55**:539–552.
544 doi:10.1080/10635150600755453

545 Anisimova M, Gil M, Dufayard J-F, Dessimoz C, Gascuel O. 2011. Survey of branch support
546 methods demonstrates accuracy, power, and robustness of fast likelihood-based
547 approximation schemes. *Systematic Biol* **60**:685–699. doi:10.1093/sysbio/syr041

548 Balmas E, Rana BM, Hamilton R, Shreeve N, Kieckbusch J, Aye I, Hawkes D, Trotter S, López-
549 Tello J, Yong HE, Valenti S, Sferruzi-Perri A, Gaccioli F, McKenzie AN, Colucci F. 2018.
550 Maternal group 2 innate lymphoid cells control fetal growth and protect from endotoxin-
551 induced abortion in mice. bioRxiv.

552 Bauernfeind AL, Zintel TM, Pizzollo J, Ely JJ, Raghanti MA, Hopkins WD, Hof PR, Sherwood
553 CC, Babbitt CC. 2021. Tempo and mode of gene expression evolution in the brain across
554 Primates. *Biorxiv* 2021.04.21.440670. doi:10.1101/2021.04.21.440670

555 Bergsten J. 2005. A review of long-branch attraction. *Cladistics* **21**:163–193.
556 doi:10.1111/j.1096-0031.2005.00059.x

557 Billington WD. 1965. THE INVASIVENESS OF TRANSPLANTED MOUSE TROPHOBLAST
558 AND THE INFLUENCE OF IMMUNOLOGICAL FACTORS. *Reproduction* **10**:343–352.
559 doi:10.1530/jrf.0.0100343

560 Blackburn DG. 2015. Evolution of vertebrate viviparity and specializations for fetal nutrition: A
561 quantitative and qualitative analysis. *J Morphol* **276**:961–990. doi:10.1002/jmor.20272

562 Blackburn DG. 1993. Histology of the late-stage placentae in the matrotrophic skink *Chalcides*
563 *chalcides* (Lacertilia; Scincidae). *J Morphol* **216**:179–195. doi:10.1002/jmor.1052160206

564 Blackburn DG, Brandley M. 2015. Viviparous placentotrophy in reptiles and the parent-offspring
565 conflict. *J Exp Zoology Part B Mol Dev Evol* **324**:532–548. doi:10.1002/jez.b.22624

566 Blackburn DG, Callard IP. 1997. Morphogenesis of placental membranes in the viviparous,
567 placentotrophic lizard *Chalcides chalcides* (Squamata: Scincidae). *J Morphol* **232**:35–55.
568 doi:10.1002/(sici)1097-4687(199704)232:1<35::aid-jmor2>3.0.co;2-n

569 Blackburn DG, Starck JM. 2015. Morphological specializations for fetal maintenance in
570 viviparous vertebrates: An introduction and historical retrospective. *J Morphol* **276**:E1–E16.
571 doi:10.1002/jmor.20410

572 Boddy AM, Abegglen LM, Pessier AP, Schiffman JD, Maley CC, Witte C. 2020. {Lifetime cancer
573 prevalence and life history traits in mammals}. *Evol Medicine Public Heal*.
574 doi:10.1093/emph/eoaa015

575 Brawand D, Soumillon M, Necsulea A, Julien P, Csardi G, Harrigan P, Weier M, Liechti A,
576 Aximu-Petri A, Kircher M, Albert FW, Zeller U, Khaitovich P, Grutzner F, Bergmann S,
577 Nielsen R, Paabo S, Kaessmann H. 2011. The evolution of gene expression levels in
578 mammalian organs. *Nature* **478**:343–348. doi:10.1038/nature10532

579 Brigandt I, Love AC. 2010. Evolutionary Novelty and the Evo-Devo Synthesis: Field Notes. *Evol*
580 *Biol* **37**:93–99. doi:10.1007/s11692-010-9083-6

581 Carter A M, Enders AC. 2004. Comparative aspects of trophoplast development and
582 placentation. *Reprod Biol Endocrin* **2**:46.

583 Carter Anthony M, Enders AC. 2004. Comparative aspects of trophoblast development and
584 placentation. *Reprod Biol Endocrin* **2**:46. doi:10.1186/1477-7827-2-46

585 Castoe TA, Koning APJ de, Kim H-M, Gu W, Noonan BP, Naylor G, Jiang ZJ, Parkinson CL,
586 Pollock DD. 2009. Evidence for an ancient adaptive episode of convergent molecular
587 evolution. *Proc National Acad Sci* **106**:8986–8991. doi:10.1073/pnas.0900233106

588 Chanderbali AS, Berger BA, Howarth DG, Soltis PS, Soltis DE. 2016. Evolving Ideas on the
589 Origin and Evolution of Flowers: New Perspectives in the Genomic Era. *Genetics* **202**:1255–
590 1265. doi:10.1534/genetics.115.182964

591 Chavan AR, Wagner GP. 2016. The fetal-maternal interface of the nine-banded armadillo:
592 endothelial cells of maternal sinus are partially replaced by trophoblast. *Zoological Lett* **2**:11.
593 doi:10.1186/s40851-016-0048-1

594 Chen C-F, Foley J, Tang P-C, Li A, Jiang TX, Wu P, Widelitz RB, Chuong CM. 2015.
595 Development, Regeneration, and Evolution of Feathers. *Annu Rev Anim Biosci* **3**:1–27.
596 doi:10.1146/annurev-animal-022513-114127

597 Christin P-A, Petitpierre B, Salamin N, Büchi L, Besnard G. 2009. Evolution of C4
598 Phosphoenolpyruvate Carboxykinase in Grasses, from Genotype to Phenotype. *Mol Biol*
599 *Evol* **26**:357–365. doi:10.1093/molbev/msn255

600 Church SH, Munro C, Dunn CW, Extavour CG. 2022. Identifying evolutionary divergence in
601 gene expression across species and organs: a case-study using Hawaiian *Drosophila*.
602 *Biorxiv* 2021.11.30.470652. doi:10.1101/2021.11.30.470652

603 Corpa JM. 2006. Ectopic pregnancy in animals and humans. *Reproduction* **131**:631–640.
604 doi:10.1530/rep.1.00606

605 Corso G, Delitala GM, Carcupino M. 2000. Uterine morphology during the annual cycle in
606 *Chalcides ocellatus tiligugu* (Gmelin) (Squamata: Scincidae). *J Morphol* **243**:153–165.
607 doi:10.1002/(sici)1097-4687(200002)243:2<153::aid-jmor4>3.0.co;2-q

608 Costanzo V, Bardelli A, Siena S, Abrignani S. 2018. Exploring the links between cancer and
609 placenta development. *Open Biol* **8**:180081. doi:10.1098/rsob.180081

610 Cui Y, Wang W, Dong N, Lou J, Srinivasan DK, Cheng W, Huang X, Liu M, Fang C, Peng J,
611 Chen S, Wu S, Liu Z, Dong L, Zhou Y, Wu Q. 2012. Role of corin in trophoblast invasion and
612 uterine spiral artery remodelling in pregnancy. *Nature* **484**:246–250.
613 doi:10.1038/nature10897

614 Elliot MG, Crespi BJ. 2009. Phylogenetic Evidence for Early Hemochorial Placentation in
615 Eutheria. *Placenta* **30**:949–967. doi:10.1016/j.placenta.2009.08.004

616 Elliot MG, Crespi BJ. 2006. Placental Invasiveness Mediates the Evolution of Hybrid Inviability
617 in Mammals. *Am Nat* **168**:114–120. doi:10.1086/505162

618 Felsenstein J. 1978. Cases in which Parsimony or Compatibility Methods will be Positively
619 Misleading. *Systematic Biol* **27**:401–410. doi:10.1093/sysbio/27.4.401

620 Ferretti C, Bruni L, Dangles-Marie V, Pecking AP, Bellet D. 2006. Molecular circuits shared by
621 placental and cancer cells, and their implications in the proliferative, invasive and migratory
622 capacities of trophoblasts. *Hum Reprod Update* **13**:121–141. doi:10.1093/humupd/dml048

623 Figuet E, Ballenghien M, Romiguier J, Galtier N. 2014. Biased Gene Conversion and GC-
624 Content Evolution in the Coding Sequences of Reptiles and Vertebrates. *Genome Biol Evol*
625 **7**:240–250. doi:10.1093/gbe/evu277

626 Freyer C, Renfree MB. 2009. The mammalian yolk sac placenta. *J Exp Zoology Part B Mol Dev*
627 *Evol* **312B**:545–554. doi:10.1002/jez.b.21239

628 Galtier N. 2001. Maximum-Likelihood Phylogenetic Analysis Under a Covarion-like Model. *Mol*
629 *Biol Evol* **18**:866–873. doi:10.1093/oxfordjournals.molbev.a003868

630 Gilad Y, Mizrahi-Man O. 2015. A reanalysis of mouse ENCODE comparative gene expression
631 data. *F1000research* **4**:121. doi:10.12688/f1000research.6536.1

632 Goldman N, Anderson JP, Rodrigo AG, Olmstead R. 2000. Likelihood-based tests of topologies
633 in phylogenetics. *Systematic Biol* **49**:652–670. doi:10.1080/106351500750049752

634 Graham CH, Lala PK. 1991. Mechanism of control of trophoblast invasion in situ. *J Cell Physiol*
635 **148**:228–234. doi:10.1002/jcp.1041480207

636 Griffith OW, Blackburn DG, Brandley MC, Dyke JUV, Whittington CM, Thompson MB. 2015.
637 Ancestral state reconstructions require biological evidence to test evolutionary hypotheses: A
638 case study examining the evolution of reproductive mode in squamate reptiles. *J Exp*
639 *Zoology Part B Mol Dev Evol* **324**:493–503. doi:10.1002/jez.b.22614

640 Griffith OW, Dyke JUV, Thompson MB. 2013. No implantation in an extra-uterine pregnancy of a
641 placentotrophic reptile. *Placenta* **34**:510–511. doi:10.1016/j.placenta.2013.03.002

642 Gu X. 2004. Statistical Framework for Phylogenomic Analysis of Gene Family Expression
643 Profiles. *Genetics* **167**:531–542. doi:10.1534/genetics.167.1.531

644 Guerrero RF, Hahn MW. 2018. Quantifying the risk of hemiplasy in phylogenetic inference. *Proc*
645 *National Acad Sci* **115**:12787–12792. doi:10.1073/pnas.1811268115

646 Guindon S, Dufayard J-F, Lefort V, Anisimova M, Hordijk W, Gascuel O. 2010. New algorithms
647 and methods to estimate maximum-likelihood phylogenies: assessing the performance of
648 PhyML 3.0. *Systematic Biol* **59**:307–321. doi:10.1093/sysbio/syq010

649 Gurchot C. 1975. The Trophoblast Theory of Cancer (John Beard, 1857–1924) Revisited.
650 *Oncology* **31**:310–333. doi:10.1159/000225037

651 Haim-Vilmsky L, Henriksson J, Walker JA, Miao Z, Natan E, Kar G, Clare S, Barlow JL,
652 Charidemou E, Mamanova L, Chen X, Proserpio V, Pramanik J, Woodhouse S, Protasio AV,
653 Efremova M, Griffin JL, Berriman M, Dougan G, Fisher J, Marioni JC, McKenzie AN,
654 Teichmann SA. 2020. Rora regulates activated T helper cells during inflammation. *Biorxiv*
655 709998. doi:10.1101/709998

656 Hibbins MS, Gibson MJ, Hahn MW. 2020. Determining the probability of hemiplasy in the
657 presence of incomplete lineage sorting and introgression. *Elife* **9**:e63753.
658 doi:10.7554/elif.63753

659 Hill JP. 1932. II. Croonian lecture. - the developmental history of the primates. *Philosophical*
660 *Transactions Royal Soc Lond Ser B Contain Pap Biological Character* **221**:45–178.
661 doi:10.1098/rstb.1932.0002

662 Hirasawa T, Kuratani S. 2015. Evolution of the vertebrate skeleton: morphology, embryology,
663 and development. *Zoological Lett* **1**:2. doi:10.1186/s40851-014-0007-7

664 Hoang DT, Chernomor O, Haeseler A von, Minh BQ, Vinh LS. 2018. UFBoot2: Improving the
665 Ultrafast Bootstrap Approximation. *Mol Biol Evol* **35**:518–522. doi:10.1093/molbev/msx281

666 Hughes RL, Hall LS. 1998. Early development and embryology of the platypus. *Philosophical*
667 *Transactions Royal Soc Lond Ser B Biological Sci* **353**:1101–1114.
668 doi:10.1098/rstb.1998.0269

669 Huhn O, Ivarsson MA, Gardner L, Hollinshead M, Stinchcombe JC, Chen P, Shreeve N,
670 Chazara O, Farrell LE, Theorell J, Ghadially H, Parham P, Griffiths G, Horowitz A, Moffett A,
671 Sharkey AM, Colucci F. 2020. Distinctive phenotypes and functions of innate lymphoid cells
672 in human decidua during early pregnancy. *Nat Commun* **11**:381. doi:10.1038/s41467-019-
673 14123-z

674 Jain A, Tuteja G. 2021. PlacentaCellEnrich: A tool to characterize gene sets using placenta cell-
675 specific gene enrichment analysis. *Placenta* **103**:164–171.
676 doi:10.1016/j.placenta.2020.10.029

677 Jollie WP. 1961. The incidence of experimentally produced abdominal implantations in the rat.
678 *Anatomical Rec* **141**:159–167. doi:10.1002/ar.1091410209

679 Kalyaanamoorthy S, Minh BQ, Wong TKF, Haeseler A von, Jermiin LS. 2017. ModelFinder: fast
680 model selection for accurate phylogenetic estimates. *Nat Methods* **14**:587–589.
681 doi:10.1038/nmeth.4285

682 Katelyn M, Mirna M, Manvendra S, Joanne M, Joris B Jan, J L Vincent. 2021. Evolutionary
683 transcriptomics implicates new genes and pathways in human pregnancy and adverse
684 pregnancy outcomes. *Elife* **10**:e69584. doi:10.7554/elife.69584

685 Kihlström JE. 1972. Period of gestation and body weight in some placental mammals. *Comp*
686 *Biochem Physiology Part Physiology* **43**:673–679. doi:10.1016/0300-9629(72)90254-x

687 Kin K, Nnamani MC, Lynch VJ, Michaelides E, Wagner GP. 2015. Cell-type Phylogenetics and
688 the Origin of Endometrial Stromal Cells. *Cell reports*.

689 Kishino H, Hasegawa M. 1989. Evaluation of the maximum likelihood estimate of the
690 evolutionary tree topologies from DNA sequence data, and the branching order in
691 hominoidea. *J Mol Evol* **29**:170–179. doi:10.1007/bf02100115

692 Kishino H, Miyata T, Hasegawa M. 1990. Maximum likelihood inference of protein phylogeny
693 and the origin of chloroplasts. *J Mol Evol* **31**:151–160. doi:10.1007/bf02109483

694 Kolaczowski B, Thornton JW. 2008. A Mixed Branch Length Model of Heterotachy Improves
695 Phylogenetic Accuracy. *Mol Biol Evol* **25**:1054–1066. doi:10.1093/molbev/msn042

696 Kostka D, Hubisz MJ, Siepel A, Pollard KS. 2012. The role of GC-biased gene conversion in
697 shaping the fastest evolving regions of the human genome. *Mol Biol Evol* **29**:1047–1057.
698 doi:10.1093/molbev/msr279

699 Kozlov AP. 2022. Mammalian tumor-like organs. 1. The role of tumor-like normal organs and
700 atypical tumor organs in the evolution of development (carcino-evo-devo). *Infect Agents*
701 *Cancer* **17**:2. doi:10.1186/s13027-021-00412-0

702 Kshitiz, Afzal J, Maziarz JD, Hamidzadeh A, Liang C, Erkenbrack EM, Kim HN, Haeger J-D,
703 Pfarrer C, Hoang T, Ott T, Spencer T, Pavličev M, Antczak DF, Levchenko A, Wagner GP.
704 2019. Evolution of placental invasion and cancer metastasis are causally linked. *Nat Ecol*
705 *Evol* **3**:1743–1753. doi:10.1038/s41559-019-1046-4

706 Lala PK, Nandi P, Hadi A, Halari C. 2021. A crossroad between placental and tumor biology:
707 What have we learnt? *Placenta* **116**:12–30. doi:10.1016/j.placenta.2021.03.003

708 Landgraf AJ, Lee Y. 2015. Dimensionality Reduction for Binary Data through the Projection of
709 Natural Parameters. *arXiv.org stat.ML*.

710 Lartillot N. 2013. Phylogenetic Patterns of GC-Biased Gene Conversion in Placental Mammals
711 and the Evolutionary Dynamics of Recombination Landscapes. *Mol Biol Evol* **30**:489–502.
712 doi:10.1093/molbev/mss239

713 Lewis PO, Olmstead R. 2001. A Likelihood Approach to Estimating Phylogeny from Discrete
714 Morphological Character Data. *Systematic Biol* **50**:913–925.
715 doi:10.1080/106351501753462876

716 Li G, Wang J, Rossiter SJ, Jones G, Cotton JA, Zhang S. 2008. The hearing gene Prestin
717 reunites echolocating bats. *Proc National Acad Sci* **105**:13959–13964.
718 doi:10.1073/pnas.0802097105

719 Li Y, Liu Z, Shi P, Zhang J. 2010. The hearing gene Prestin unites echolocating bats and
720 whales. *Curr Biol* **20**:R55–R56. doi:10.1016/j.cub.2009.11.042

721 Liang C, Musser JM, Cloutier A, Prum RO, Wagner GP. 2018. Pervasive Correlated Evolution in
722 Gene Expression Shapes Cell and Tissue Type Transcriptomes. *Genome Biol Evol* **10**:538–
723 552. doi:10.1093/gbe/evy016

724 Liu Y, Cotton JA, Shen B, Han X, Rossiter SJ, Zhang S. 2010. Convergent sequence evolution
725 between echolocating bats and dolphins. *Curr Biol* **20**:R53–R54.
726 doi:10.1016/j.cub.2009.11.058

727 Loeb L. 1914. The experimental production of an early stage of extrauterine pregnancy. *P Soc*
728 *Exp Biol Med* **11**:103–106. doi:10.3181/00379727-11-64

729 Luckett P. 1976. Cladistic Relationships among Primate Higher Categories: Evidence of the
730 Fetal Membranes and Placenta. *Folia Primatol* **25**:245–276. doi:10.1159/000155719

731 Luckett WP. 1975. Phylogeny of the Primates, A Multidisciplinary Approach 157–182.
732 doi:10.1007/978-1-4684-2166-8_7

733 Luckett WP. 1974. Comparative development and evolution of the placenta in primates. *Contrib*
734 *Primatol* **3**:142–234.

735 Lynch VJ. 2022. Evolution: Stress fans the flames of innovation. *Curr Biol* **32**:R158–R160.
736 doi:10.1016/j.cub.2022.01.030

737 Lynch VJ, Nnamani MC, Kapusta A, Brayer K, Plaza SL, Mazur EC, Emera D, Sheikh SZ,
738 Grutzner F, Bauersachs S. 2015. Ancient transposable elements transformed the uterine
739 regulatory landscape and transcriptome during the evolution of mammalian pregnancy. *Cell*
740 *reports* **10**:551–561.

741 Lyson TR, Bever GS. 2020. Origin and Evolution of the Turtle Body Plan. *Annu Rev Ecol Evol*
742 *Syst* **51**:1–24. doi:10.1146/annurev-ecolsys-110218-024746

743 Lyu M, Suzuki H, Kang L, Gaspal F, Zhou W, Goc J, Zhou L, Zhou J, Zhang W, Bank JLC, Shen
744 Z, Fox JG, Sockolow RE, Laufer TM, Fan Y, Eberl G, Withers DR, Sonnenberg GF. 2022.
745 ILC3s select for RORyt+ Tregs and establish tolerance to intestinal microbiota. *Biorxiv*
746 2022.04.25.489463. doi:10.1101/2022.04.25.489463

747 Maddison WP, Knowles LL. 2006. Inferring Phylogeny Despite Incomplete Lineage Sorting.
748 *Systematic Biol* **55**:21–30. doi:10.1080/10635150500354928

- 749 Maddison WP, Midford PE, Otto SP. 2007. Estimating a Binary Character's Effect on Speciation
750 and Extinction. *Systematic Biol* **56**:701–710. doi:10.1080/10635150701607033
- 751 Manzo G. 2019. Similarities Between Embryo Development and Cancer Process Suggest New
752 Strategies for Research and Therapy of Tumors: A New Point of View. *Frontiers Cell Dev*
753 *Biology* **7**:20. doi:10.3389/fcell.2019.00020
- 754 Marinić M, Mika K, Chigurupati S, Lynch VJ. 2021. Evolutionary transcriptomics implicates
755 HAND2 in the origins of implantation and regulation of gestation length. *Elife* **10**:e61257.
756 doi:10.7554/elife.61257
- 757 Martin RD. 2008. Evolution of Placentation in Primates: Implications of Mammalian Phylogeny.
758 *Evol Biol* **35**:125–145. doi:10.1007/s11692-008-9016-9
- 759 Martin RD. 1969. The evolution of reproductive mechanisms in primates. *J Reprod Fertil Suppl*
760 49–66.
- 761 McGowen MR, Erez O, Romero R, Wildman DE. 2014. The evolution of embryo implantation.
762 *Int J Dev Biol* **58**:155–161. doi:10.1387/ijdb.140020dw
- 763 Mendes J, Areia AL, Rodrigues-Santos P, Santos-Rosa M, Mota-Pinto A. 2020. Innate
764 Lymphoid Cells in Human Pregnancy. *Front Immunol* **11**:551707.
765 doi:10.3389/fimmu.2020.551707
- 766 Mendes J, Rodrigues-Santos P, Areia AL, Almeida J-S, Alves V, Santos-Rosa M, Mota-Pinto A.
767 2021. Type 2 and type 3 innate lymphoid cells at the maternal-fetal interface: implications in
768 preterm birth. *Bmc Immunol* **22**:28. doi:10.1186/s12865-021-00423-x
- 769 Mess A, Carter AM. 2006. Evolutionary transformations of fetal membrane characters in
770 Eutheria with special reference to Afrotheria. *J Exp Zoology Part B Mol Dev Evol* **306B**:140–
771 163. doi:10.1002/jez.b.21079
- 772 Mika K, Marinić M, Singh M, Lynch VJ. 2021. Evolutionary transcriptomics implicates new genes
773 and pathways in human pregnancy and adverse pregnancy outcomes. *Biorxiv*
774 2021.04.19.440514. doi:10.1101/2021.04.19.440514
- 775 Miller D, Motomura K, Garcia-Flores V, Romero R, Gomez-Lopez N. 2018. Innate Lymphoid
776 Cells in the Maternal and Fetal Compartments. *Front Immunol* **9**:2396.
777 doi:10.3389/fimmu.2018.02396
- 778 Minh BQ, Schmidt HA, Chernomor O, Schrempf D, Woodhams MD, von HA. 2020. IQ-TREE 2:
779 New Models and Efficient Methods for Phylogenetic Inference in the Genomic Era. *Mol Biol*
780 *Evol* **37**:1530–1534. doi:10.1093/molbev/msaa015
- 781 Minot CS. 1891. A Theory of the Structure of the Placenta. *Anatomischer Anzeiger* **Bd 6**:125–
782 131.
- 783 Mohammadi S, Yang L, Harpak A, Herrera-Álvarez S, Rodríguez-Ordoñez M del P, Peng J,
784 Zhang K, Storz JF, Dobler S, Crawford AJ, Andolfatto P. 2021. Concerted evolution reveals

785 co-adapted amino acid substitutions in Na⁺K⁺-ATPase of frogs that prey on toxic toads. *Curr*
786 *Biol* **31**:2530-2538.e10. doi:10.1016/j.cub.2021.03.089

787 Mossman 1898- Harland W. (Harland Winfield). 1937. Comparative morphogenesis of the fetal
788 membranes and accessory uterine structures, by Harland W. Mossman ... With twenty-four
789 plates and twelve text-figures. Washington.

790 Munro C, Zapata F, Howison M, Siebert S, Dunn CW. 2021. Evolution of gene expression
791 across species and specialized zooids in Siphonophora. *Biorxiv* 2021.07.30.454354.
792 doi:10.1101/2021.07.30.454354

793 Murray M, Lessey B. 1999. Embryo Implantation and Tumor Metastasis: Common Pathways of
794 Invasion and Angiogenesis. *Semin Reprod Endocr* **17**:275–290. doi:10.1055/s-2007-
795 1016235

796 Necsulea A, Soumillon M, Warnefors M, Liechti A, Daish T, Zeller U, Baker JC, Grutzner F,
797 Kaessmann H. 2014. The evolution of lncRNA repertoires and expression patterns in
798 tetrapods. *Nature* **505**:635–640.

799 Newman AM, Steen CB, Liu CL, Gentles AJ, Chaudhuri AA, Scherer F, Khodadoust MS,
800 Esfahani MS, Luca BA, Steiner D, Diehn M, Alizadeh AA. 2019. Determining cell type
801 abundance and expression from bulk tissues with digital cytometry. *Nat Biotechnol* **37**:773–
802 782. doi:10.1038/s41587-019-0114-2

803 Nguyen L-T, Schmidt HA, Haeseler A von, Minh BQ. 2015. IQ-TREE: A Fast and Effective
804 Stochastic Algorithm for Estimating Maximum-Likelihood Phylogenies. *Mol Biol Evol* **32**:268–
805 274. doi:10.1093/molbev/msu300

806 Nordor AV, Nehar-Belaid D, Richon S, Klatzmann D, Bellet D, Dangles-Marie V, Fournier T,
807 Aryee MJ. 2017. The early pregnancy placenta foreshadows DNA methylation alterations of
808 solid tumors. *Epigenetics* **12**:793–803. doi:10.1080/15592294.2017.1342912

809 Oksanen J, Kindt R, Legendre P, O'Hara B, Simpson GL, Solymos P, Stevens MHH, Wagner H.
810 2008. vegan: Community Ecology Package.

811 Pagel M. 1999. The Maximum Likelihood Approach to Reconstructing Ancestral Character
812 States of Discrete Characters on Phylogenies. *Systematic Biol* **48**:612–622.
813 doi:10.1080/106351599260184

814 Pal S, Oliver B, Przytycka TM. 2021. Modeling gene expression evolution with EvoGeneX
815 uncovers differences in evolution of species, organs and sexes. *Biorxiv* 2020.01.06.895615.
816 doi:10.1101/2020.01.06.895615

817 Perry JK, Lins RJ, Lobie PE, Mitchell MD. 2009. Regulation of invasive growth: similar
818 epigenetic mechanisms underpin tumour progression and implantation in human pregnancy.
819 *Clin Sci* **118**:451–457. doi:10.1042/cs20090503

820 Philippe H, Zhou Y, Brinkmann H, Rodrigue N, Delsuc F. 2005. Heterotachy and long-branch
821 attraction in phylogenetics. *Bmc Evol Biol* **5**:50. doi:10.1186/1471-2148-5-50

822 Piechowski J. 2019. Plausibility of trophoblastic-like regulation of cancer tissue. *Cancer*
823 *Management Res* **11**:5033–5046. doi:10.2147/cmar.s190932

824 Portmann A. 1938. Die Ontogenese der Säugetiere als Evolutionsproblem. S. Karger.

825 Price PD, Droguett DHP, Taylor JA, Kim DW, Place ES, Rogers TF, Mank JE, Cooney CR,
826 Wright AE. 2022. Detecting signatures of selection on gene expression. *Nat Ecol Evol* 1–11.
827 doi:10.1038/s41559-022-01761-8

828 Renfree M, Shaw G. 2013. eLS. doi:10.1038/npg.els.0001856

829 Renfree MB. 2010. Review: Marsupials: Placental Mammals with a Difference. *Placenta*
830 **31**:S21–S26. doi:10.1016/j.placenta.2009.12.023

831 Romiguier J, Ranwez V, Delsuc F, Galtier N, Douzery EJP. 2013. Less Is More in Mammalian
832 Phylogenomics: AT-Rich Genes Minimize Tree Conflicts and Unravel the Root of Placental
833 Mammals. *Mol Biol Evol* **30**:2134–2144. doi:10.1093/molbev/mst116

834 Ross CA. 2014. The Trophoblast Model of Cancer. *Nutrition Cancer* **67**:61–67.
835 doi:10.1080/01635581.2014.956257

836 Samuel CA, Perry JS. 1972. The ultrastructure of pig trophoblast transplanted to an ectopic site
837 in the uterine wall. *J Anat* **113**:139–49.

838 Shimodaira H. 2002. An Approximately Unbiased Test of Phylogenetic Tree Selection.
839 *Systematic Biol* **51**:492–508. doi:10.1080/10635150290069913

840 Soubrier J, Steel M, Lee MSY, Sarkissian CD, Guindon S, Ho SYW, Cooper A. 2012. The
841 Influence of Rate Heterogeneity among Sites on the Time Dependence of Molecular Rates.
842 *Mol Biol Evol* **29**:3345–3358. doi:10.1093/molbev/mss140

843 Strimmer K, Rambaut A. 2002. Inferring confidence sets of possibly misspecified gene trees.
844 *Proc Royal Soc Lond Ser B Biological Sci* **269**:137–142. doi:10.1098/rspb.2001.1862

845 Swanson P, Skinner MK. 2018. Encyclopedia of Reproduction 1–2. doi:10.1016/b978-0-12-
846 811899-3.20528-4

847 Teeling EC. 2009. Hear, hear: the convergent evolution of echolocation in bats? *Trends Ecol*
848 *Evol* **24**:351–354. doi:10.1016/j.tree.2009.02.012

849 Thompson A, May MR, Moore BR, Kopp A. 2020. A hierarchical Bayesian mixture model for
850 inferring the expression state of genes in transcriptomes. *P Natl Acad Sci Usa* **117**:19339–
851 19346. doi:10.1073/pnas.1919748117

852 Tung P-Y, Blischak JD, Hsiao CJ, Knowles DA, Burnett JE, Pritchard JK, Gilad Y. 2017. Batch
853 effects and the effective design of single-cell gene expression studies. *Sci Rep-uk* **7**:39921.
854 doi:10.1038/srep39921

855 Turner W. 1876. Some general observations on the placenta, with
856 special reference to the theory of evolution. *J Anat Physiol* 33–53.

857 Vento-Tormo R, Efremova M, Botting RA, Turco MY, Vento-Tormo M, Meyer KB, Park J-E,
858 Stephenson E, Polański K, Goncalves A, Gardner L, Holmqvist S, Henriksson J, Zou A,
859 Sharkey AM, Millar B, Innes B, Wood L, Wilbrey-Clark A, Payne RP, Ivarsson MA, Lisgo S,
860 Filby A, Rowitch DH, Bulmer JN, Wright GJ, Stubbington MJT, Haniffa M, Moffett A,
861 Teichmann SA. 2018. Single-cell reconstruction of the early maternal-fetal interface in
862 humans. *Nature* **563**:347–353.

863 Vogel P. 2005. The current molecular phylogeny of Eutherian mammals challenges previous
864 interpretations of placental evolution. *Placenta* **26**:591–596.
865 doi:10.1016/j.placenta.2004.11.005

866 Wagner GP. 2001. What is the promise of developmental evolution? Part II: A causal
867 explanation of evolutionary innovations may be impossible. *Journal of Experimental Zoology*.

868 Wagner GP. 2000. What is the promise of developmental evolution. Part I. Why is
869 developmental biology necessary to explain evolutionary innovations? *J Exp Zool (Mol Dev*
870 *Evol)* **288**:95–98.

871 Wagner GP, Kshitiz, Dighe A, Levchenko A. 2021. The Coevolution of Placentation and Cancer.
872 *Annu Rev Anim Biosci* **10**:1–21. doi:10.1146/annurev-animal-020420-031544

873 Wagner GP, Kshitiz K, Levchenko A. 2020. Comments on Boddy et al. 2020: Available data
874 suggest positive relationship between placental invasion and malignancy. *Evol Medicine*
875 *Public Heal* **2020**:211–214. doi:10.1093/emph/eoaa024

876 Wagner GP, Larsson HCE. 2003. What is the promise of developmental evolution? III. The
877 crucible of developmental evolution. *J Exp Zoology Part B Mol Dev Evol* **300B**:1–4.
878 doi:10.1002/jez.b.41

879 Wildman DE, Chen C, Erez O, Grossman LI, Goodman M, Romero R. 2006. Evolution of the
880 mammalian placenta revealed by phylogenetic analysis. *P Natl Acad Sci Usa* **103**:3203–
881 3208. doi:10.1073/pnas.0511344103

882 Wislocki GB. 1929. On the placentation of primates, with a consideration of the phylogeny of the
883 placenta. Carnegie Institution.

884 Xu Y, Romero R, Miller D, Silva P, Panaitescu B, Theis KR, Arif A, Hassan SS, Gomez-Lopez
885 N. 2018. Innate lymphoid cells at the human maternal-fetal interface in spontaneous
886 preterm labor. *Am J Reprod Immunol* **79**:e12820. doi:10.1111/aji.12820

887 Yang J, Ruan H, Zou Y, Su Z, Gu X. 2020. Ancestral transcriptome inference based on RNA-
888 Seq and ChIP-seq data. *Methods* **176**:99–105. doi:10.1016/j.ymeth.2018.11.010

889 Yang Z. 1994. Maximum likelihood phylogenetic estimation from DNA sequences with variable
890 rates over sites: Approximate methods. *J Mol Evol* **39**:306–314. doi:10.1007/bf00160154

Yang Z. 1993. Maximum-likelihood estimation of phylogeny from DNA sequences when substitution rates differ over sites. *Mol Biol Evol* **10**:1396–401. doi:10.1093/oxfordjournals.molbev.a040082

Figure 1. Evolution and arrangement of the maternal-fetal interface and degree of placental invasion in viviparous Amniotes.

(A) Phylogenetic relationships among amniote lineages, mammalian lineages labeled. Major evolutionary steps in the evolution of pregnancy are shown for Mammalia, Theria, and Eutheria.

(B) Placenta classification based on the arraignment of the maternal-fetal interface and degree of invasiveness. Epitheliochorial placenta, in which placental invasion does not occur and the barrier between maternal blood and the chorion (tan cells) consists of maternal vascular endothelium (red cells) and uterine epithelium (blue cells).

Endotheliochorial placenta, in which the placenta invades through the uterine epithelium and the barrier between maternal blood and the chorion consists of the maternal vascular endothelium. Hemochorial placenta, in which the placenta invades through both the uterine epithelium and vascular endothelium, and maternal blood directly bathes the chorionic villi. Examples of species with each type of placenta are also shown. While the egg passes through the glandular uterine portion of the oviduct in oviparous species, the immunologically inert shell (black) prevents direct contact between maternal and fetal tissues.

Figure 2. Binary encoding uncovers phylogenetic signal in transcriptome data.

- (A) Upper, Principal Component Analysis (PCA) of gene expression levels (TPMs) grouped species randomly, consistent with significant noise. Lower, scree plot showing percent of variance explained by dimensions 1-10. Note that the flat curve of variance explained indicates there are no significant dimensions to the PCA.
- (B) Upper, logistic PCA of the binary encoded endometrial transcriptome dataset groups species by phylogenetic relatedness, indicating significant noise reduction in the binary encoded dataset. Lower, scree plot showing percent of variance explained by dimensions 1-10. Note that the "elbow" of the graph is around dimension 4, suggesting that dimensions 1-4 of the PCA are significant.

Figure 2–Source data file 1. Species names (common and binomial), genome annotations used for RNA-Seq analysis and parity mode.

Figure 2–Source data file 2. Binary encoded endometrial transcriptome dataset.

Figure 3. Maximum-likelihood (ML) phylogeny of binary encoded endometrial transcriptome data.

- (A) ML phylogeny of binary encoded endometrial transcriptome data inferred by IQ-TREE under the GTR2+FO+R3 model. Highly-supported branch splits, i.e., those with SH-aLRT \geq 80%, LBoot \geq 90%, aBayes \geq 0.90, UFboot \geq 95%, StdBoot support \geq 80%, and parametric aLRT \geq 0.95, are shown with black circles. Branch splits that are highly-supported by at least 4 of 6 methods are shown with gray circles. Particularly discordant phylogenetic relationships are shown in bold. Oviparous species are in black, viviparous species with epitheliochorial placentas in blue, endotheliochorial placentas in orange, and hemochorial placentas in red. Lizard

species are shown with genus names in italics.

(B) Phylogenetic relationships of species in (A). Discordant phylogenetic relationships compared to the ML tree are shown in bold.

(C) Tree topology tests comparing the maximum likelihood tree (GTR2+FO+H4) shown in panel A to alternate trees that correct the phylogenetic placement of specific species or the species tree shown in panel B. Delta Log L: log L difference from the maximal Log L in the set (A). bp-RELL: bootstrap proportion using RELL method. p-KH: p-value of one sided Kishino-Hasegawa test. p-SH: p-value of Shimodaira-Hasegawa test. p-WKH: p-value of weighted KH test. p-WSH: p-value of weighted SH test. c-ELW: Expected Likelihood Weight. p-AU: p-value of approximately unbiased (AU) test. + indicates tree is within the 95% confidence sets, – significant exclusion of tree from the 95% confidence sets. All tests performed 100000 resamplings using the RELL method.

Figure 3—figure supplement 1. ML phylogeny of binary encoded endometrial transcriptome data inferred by IQ-TREE under the best-fitting GTR2+FO+R3 model. Branch supports are shown for SH-aLRT (%) / LBoot (%) / aBayes / UFBoot (%) / StdBoot (%) / parametric aLRT. Clades are considered highly-supported if its SH-aLRT \geq 80%, LBoot \geq 90%, aBayes \geq 0.90, UFboot \geq 95%, StdBoot support \geq 80%, and parametric aLRT \geq 0.95. Particularly discordant phylogenetic relationships are shown in bold. Oviparous species are in black, viviparous species with epitheliochorial placentas in blue, endotheliochorial placentas in orange, and hemochorial placentas in red. Lizard species are shown with genus names in italics.

Figure 4. Fuzzy C-Means clustering of extant and ancestral transcriptomes.

(A) Species phylogeny with extant species and ancestral lineages colored according to

Fuzzy C-Means cluster membership ($K=2-6$) shown in (B). Note that ancestral nodes are numbered. Lizard species are shown with genus names in italics.

(B) Fuzzy C-Means clustering of extant and ancestral transcriptomes ($K=2-6$). Extant species and ancestral lineages colored according to maximum degree of cluster membership shown in (C). Lizard species are shown with genus names in italics.

(C) Fuzzy C-Means cluster membership of extant and ancestral transcriptomes ($K=2-6$). Degree of cluster membership is shown as a 100% stacked bar and colored according to proportion of membership in each cluster. Lizard species are shown with genus names.

Figure 4—figure supplement 1. Exploratory clustering of extant and ancestral binary encoded transcriptomes, including: 1) Exponential Family Principal Component Analysis (PCA); 2) Logistic Principal Component Analysis (LPCA); 3) Uniform Manifold Approximation and Projection (UMAP); 4) t-distributed stochastic neighbor embedding (t-SNE); and 5) Hierarchical clustering (Manhattan distances).

Figure 4—figure supplement 2. Exploratory analyses of Fuzzy C-Means cluster number.

(A) FCM cluster number estimate using the elbow plot method with $K=1-20$, which was uninformative in choosing the optimal number of clusters.

(B) Exploratory analyses of Fuzzy C-Means cluster number using the clustree method with $K=1-11$. In this figure the size of each node corresponds to the number of samples in each cluster, and the arrows colored according to the number of samples in each cluster. Transparent arrows (the incoming node proportion), show how samples from move between lower and higher cluster numbers and can be used as an indicator of cluster instability. In this graph samples switch clusters between $K=1-5$, are stable between $K=6-9$, and unstable with more than 9 clusters. These data indicate that 6 clusters is optimal for resolution, i.e., more than 6 clusters no longer provides informative cluster memberships, while more than $K \geq 9$ is over-clustered.

Figure 5. Convergent loss of *RORA* expression in species with epitheliochorial placentas.

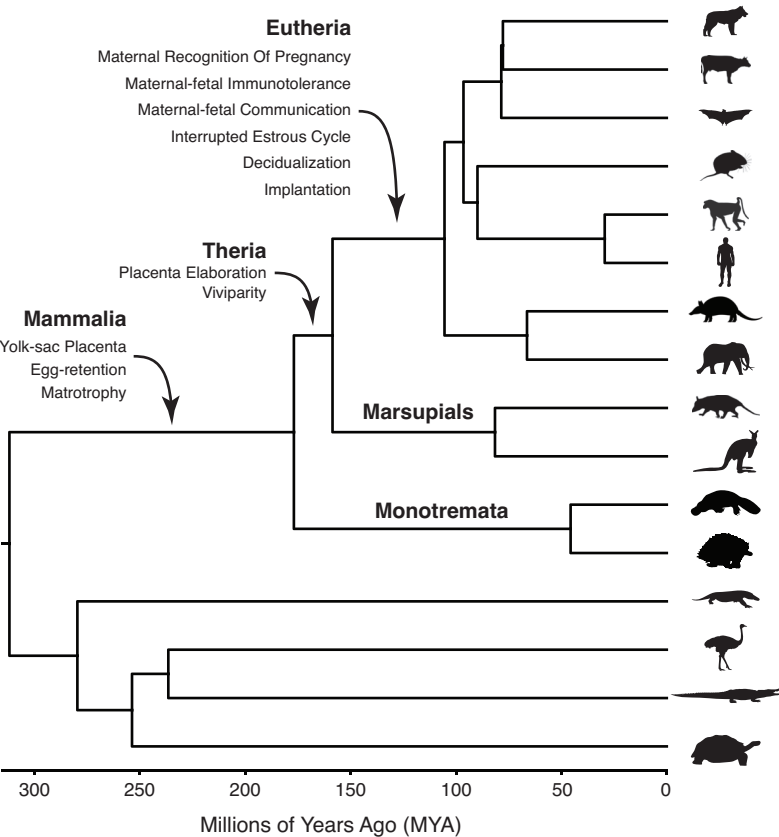
(A) Ancestral reconstruction of *RORA* expression. Pie charts at each internal node indicate the Bayesian Posterior Probability (BPP) that *RORA* is expressed (state 1, black) or not expressed (state 0, gray) at that node. Extant species are colored according to *RORA* expression ($TPM \geq 2$ = expressed, black; $TPM < 2$ = not

expressed, gray); note that the *RORA* is not annotated in the dunnart genome and is therefore indicated as “?”. Degree of placental invasiveness is shown for extant species: Hemochorial (red), endotheliochorial (orange), epitheliochorial (blue), oviparous (black). Inference of an endometrial population of ILC2/3 cells from deconvolution of bulk RNA-Seq datasets from each species is shown for extant species: Species with ILC2/3 cells and *RORA* expression (blue dots), species without ILC2/3 cells and *RORA* expression (yellow dots), and species without ILC2/3 cells and without *RORA* expression (white).

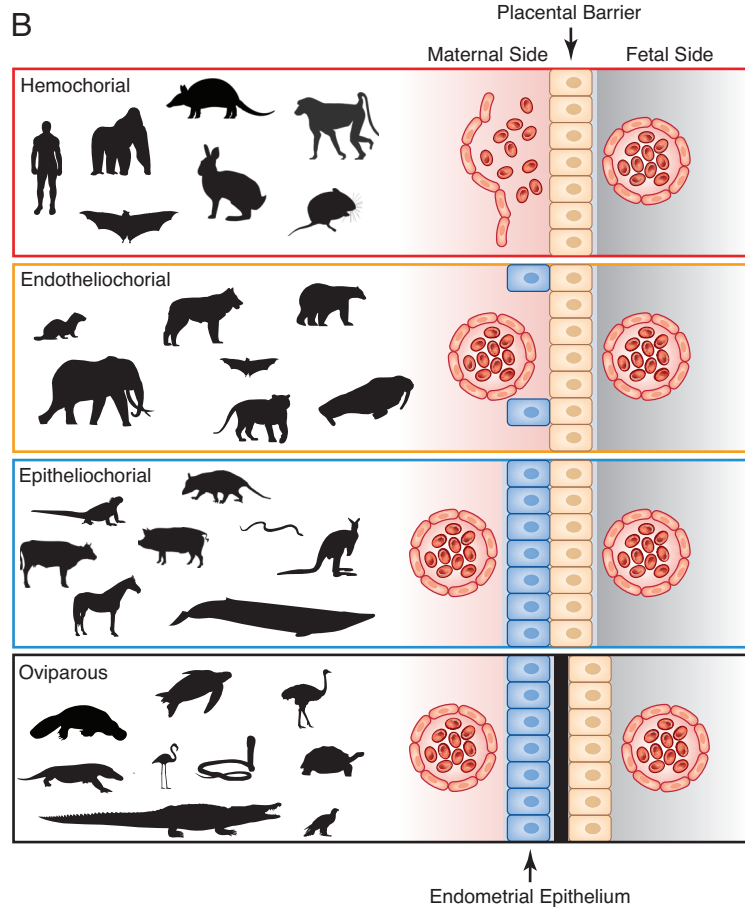
(B) *RORA* expression in single-cell RNA-Seq data from cell-types at the first trimester human maternal-fetal interface. Expression data is shown as a violin plot of log transformed counts for each cell-type. Cell-types are color coded by their location at the maternal-fetal interface: Blood (grey), decidua (pink), placenta (embryonic chorion, green).

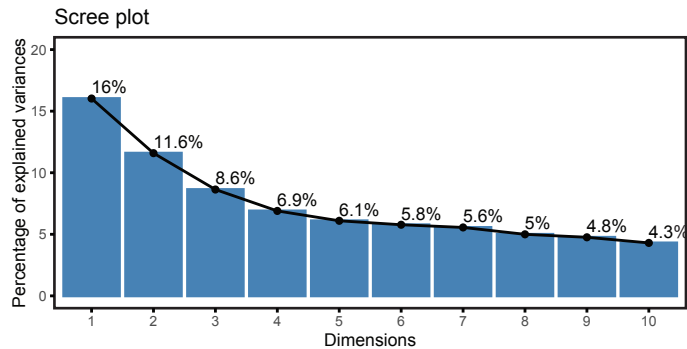
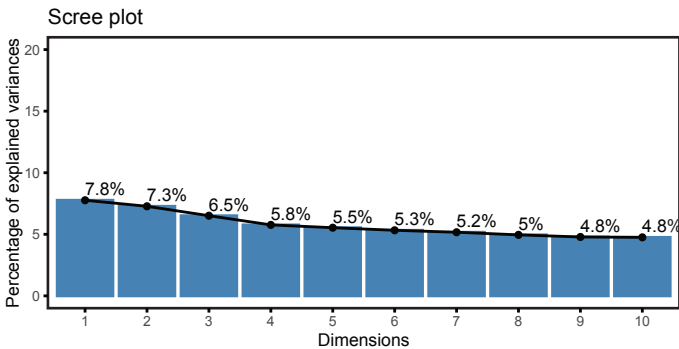
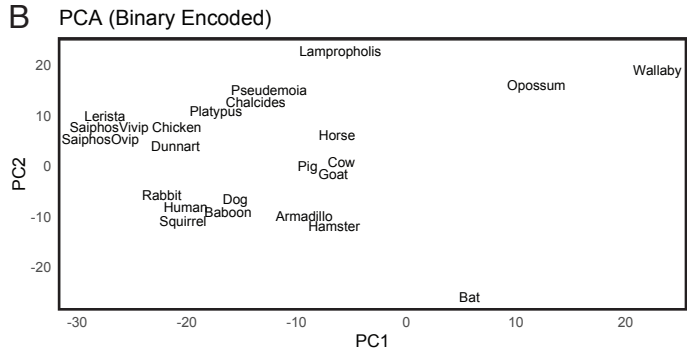
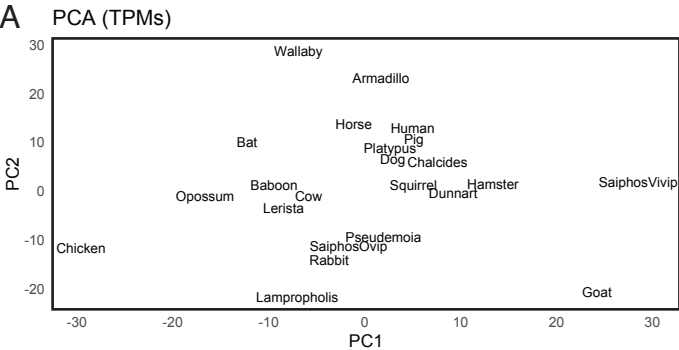
Figure 5 – source data 1. Nexus file of the binary encoded endometrial transcriptome dataset with gene names and species phylogeny.

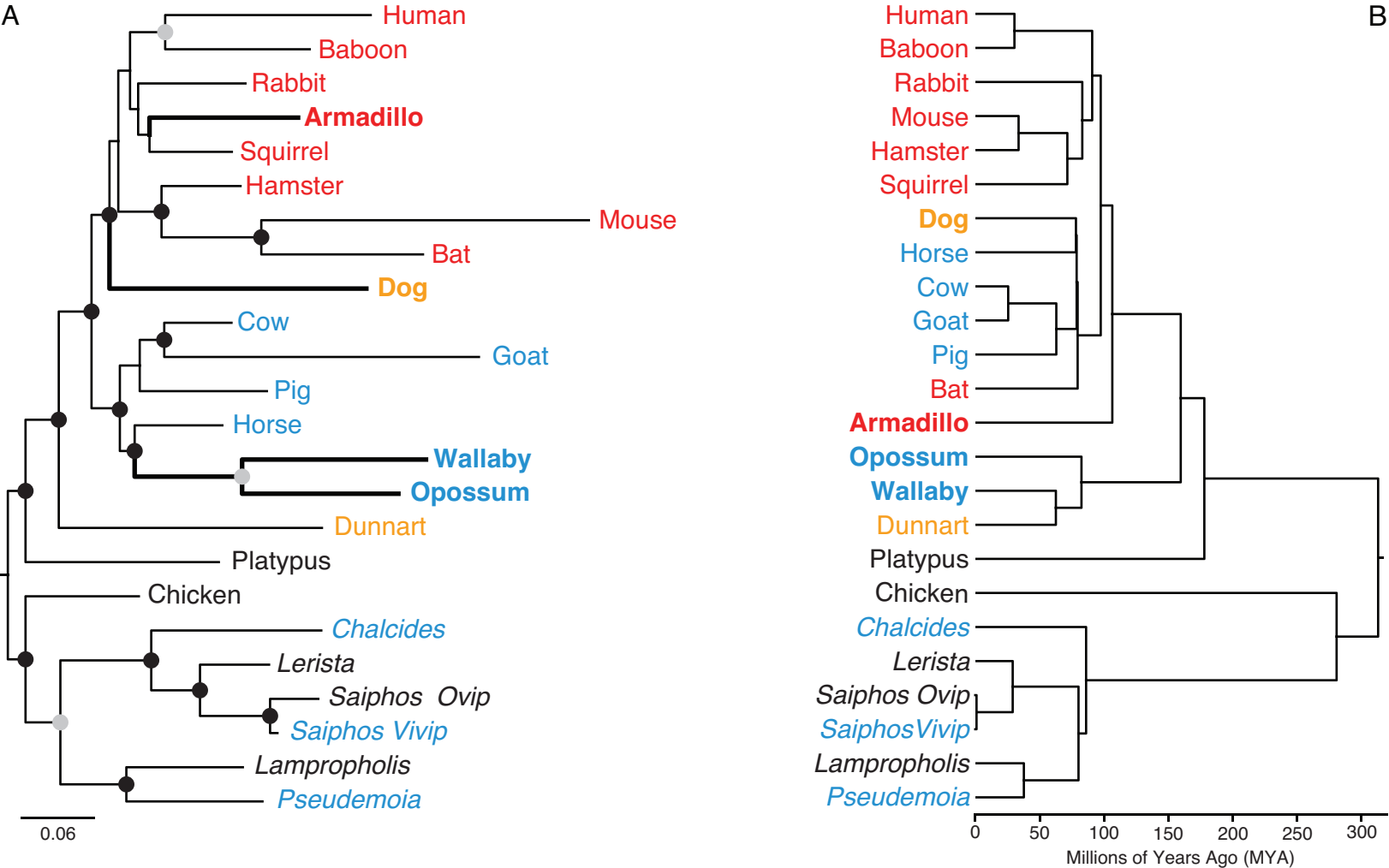
A



B

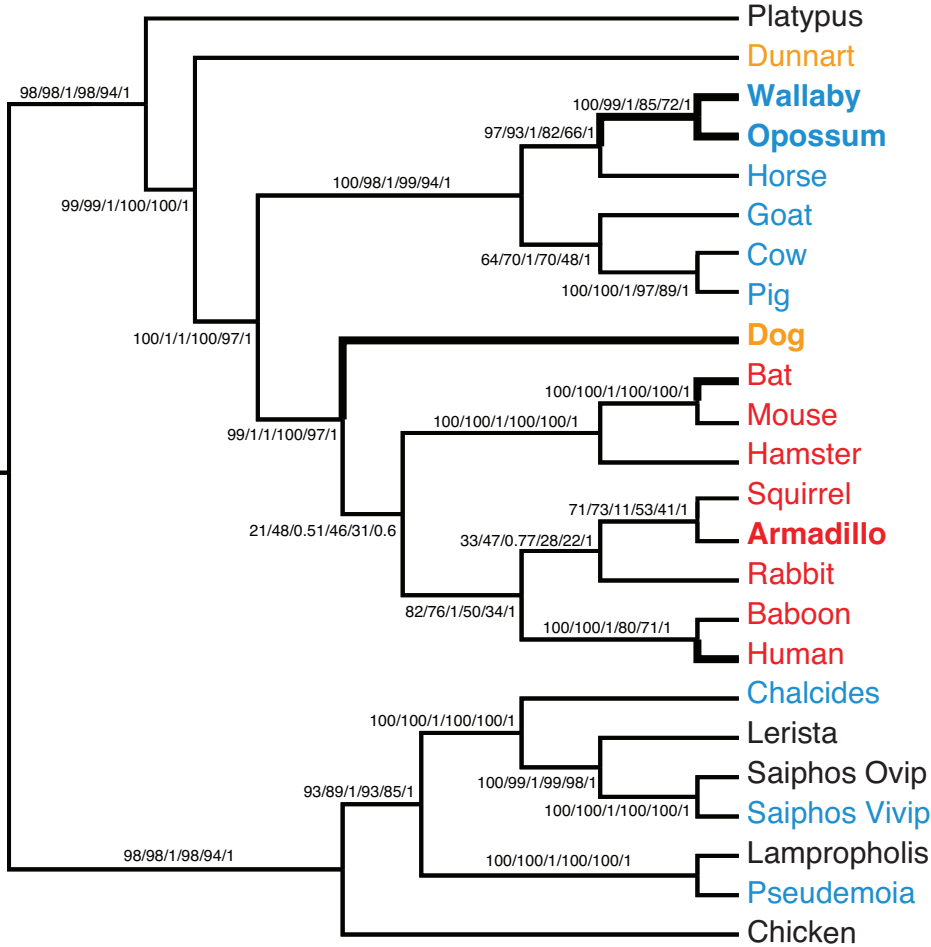




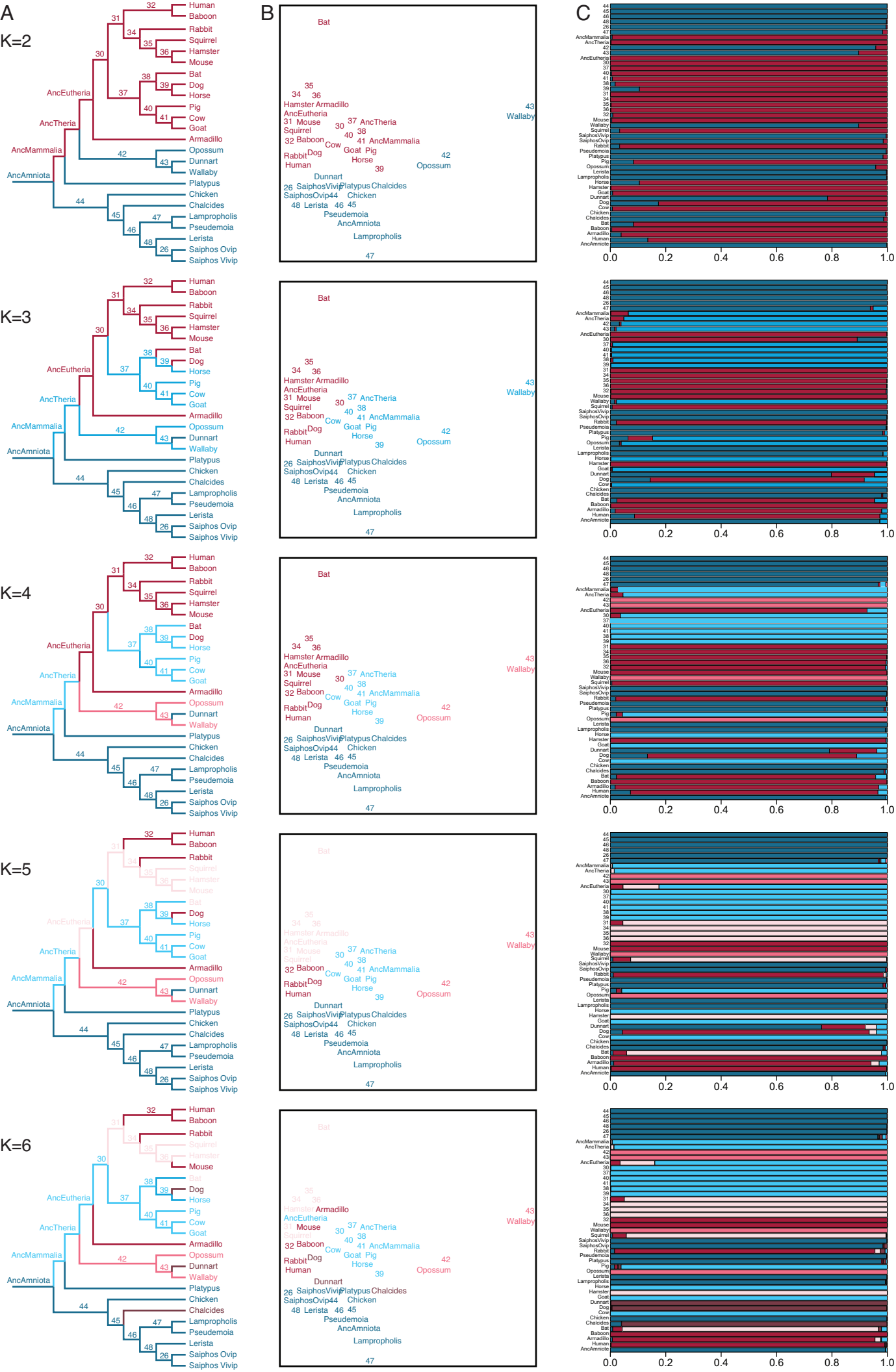


C

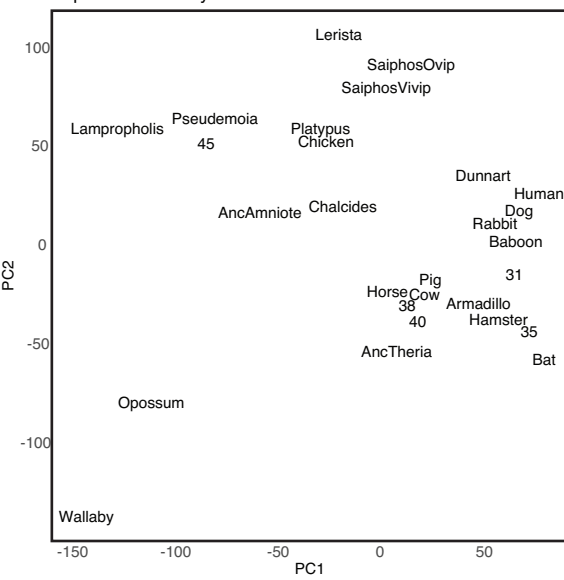
Tree	Log L	Δ Log L	bp-RELL	p-KH	p-SH	p-WKH	p-WSH	c-ELW	p-AU
Maximum Likelihood (A)	-118348.54	0.00	1.00 +	1.00 +	1.00 +	1.00 +	1.00 +	1.00 +	1.00 +
Correct Dog	-118395.01	46.47	0.003 -	0.004 -	0.22 +	0.004 -	0.016 -	0.004 -	0.003 -
Correct Bat	-118449.02	100.47	0 -	0 -	0.008 -	0 -	0 -	2.5e -21 -	4.9e -56 -
Correct Armadillo	-118514.13	165.59	0 -	0 -	1e -05 -	0 -	0 -	4.8e -30 -	1.4e -66 -
Correct Marsupials	-118568.37	219.83	0 -	0 -	0 -	0 -	0 -	5. e -50 -	4.3e -07 -
Species Tree (B)	-118978.23	629.69	0 -	0 -	0 -	0 -	0 -	1.1e -196 -	1.4e -130 -



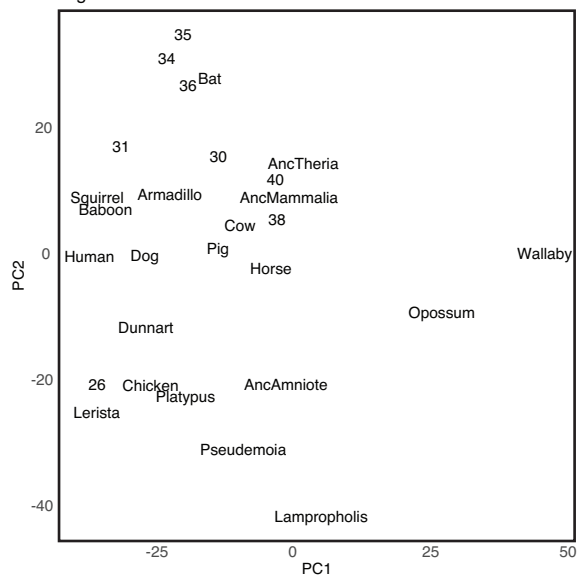
SH-aLRT (%) / LBoot (%) / aBayes / UFBoot (%) / StdBoot (%) / parametric aLRT



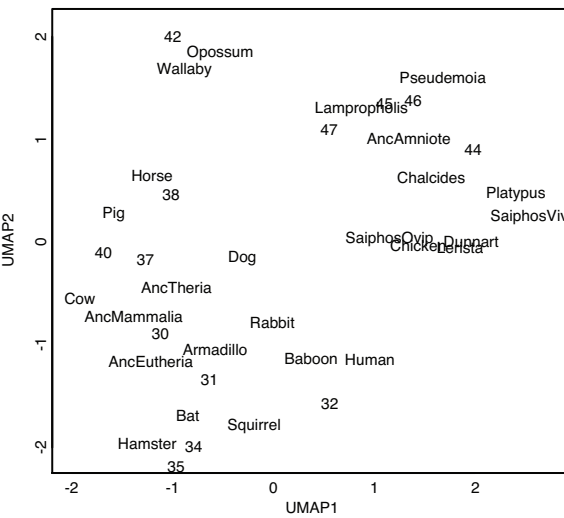
Exponential Family PCA



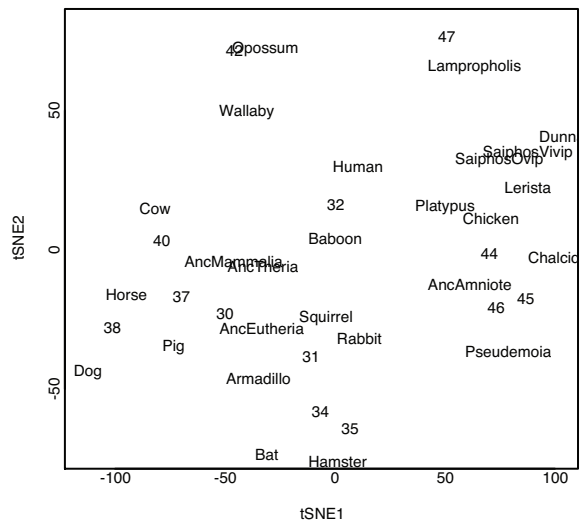
Logistic PCA



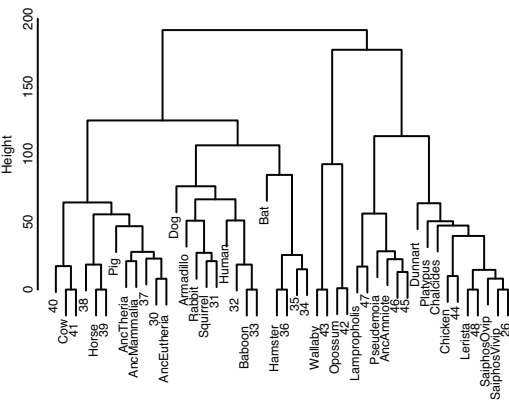
UMAP



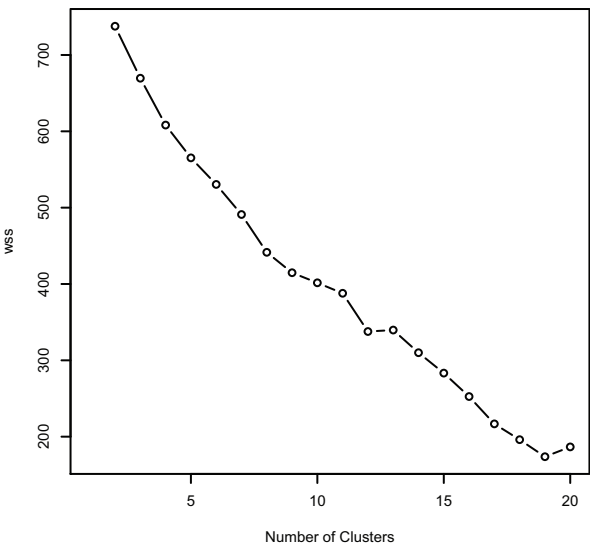
tSNE



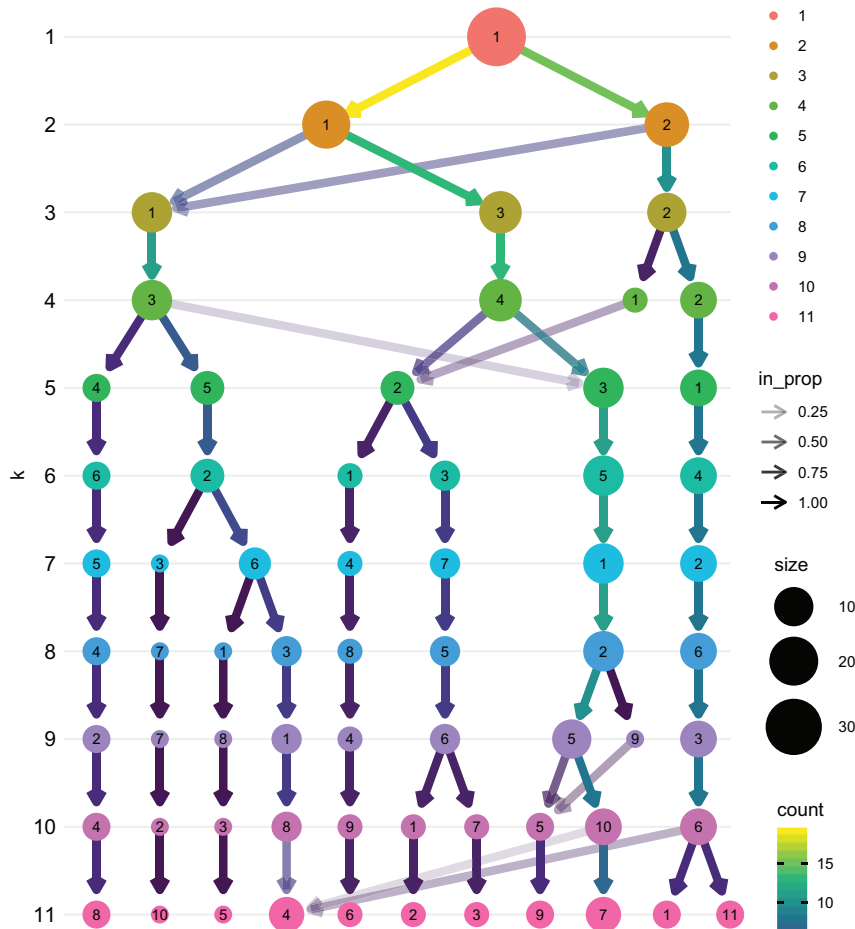
Cluster Dendrogram



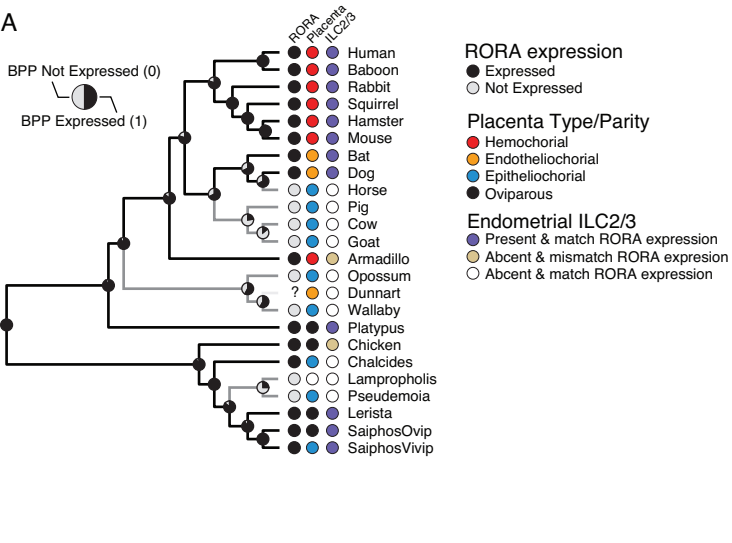
A



B



A



B

